

71

# A NOVEL ADAPTIVE FINITE ELEMENT METHOD APPLIED TO HEAT TRANSFER AND FLUID MECHANICS PROBLEMS

BY

MEDEPALLI S. M. KRISHNA

ME  
1987  
M  
KRI  
NOV

Th  
ME/1987/4  
K8977



DEPARTMENT OF MECHANICAL ENGINEERING

INDIAN INSTITUTE OF TECHNOLOGY, KANPUR

AUGUST, 1987

# **A NOVEL ADAPTIVE FINITE ELEMENT METHOD APPLIED TO HEAT TRANSFER AND FLUID MECHANICS PROBLEMS**

A Thesis Submitted  
In Partial Fulfilment of the Requirements  
for the Degree of

**MASTER OF TECHNOLOGY**

**BY**

**MEDEPALLI S. M. KRISHNA**

to the

**DEPARTMENT OF MECHANICAL ENGINEERING**

**INDIAN INSTITUTE OF TECHNOLOGY, KANPUR**

**AUGUST, 1987**

The first  
edition was  
1880.

ME-1987-M-KRI-NOV

CERTIFICATE

It is certified that the thesis entitled,  
'A Novel Adaptive Finite Element Technique Applied to  
Heat Transfer and Fluid Mechanics Problems" has been  
carried out by Medepalli S.M. Krishna under my super-  
vision and that it has not been submitted elsewhere  
for the award of a degree.

July, 1987

(Dr. T. Sundararajan)  
Assistant Professor  
Department of Mechanical Engineering  
Indian Institute of Technology  
KANPUR



To my dear brothers

Sudha and Giri

## ACKNOWLEDGEMENTS

I deeply express my gratitude to my supervisor Dr. T. Sundararajan without whose support this work could not have been done. I thank him very much for his enthusiasm in this area of research and the encouragement he gave at every step of the research.

I also thank Dr. P.C. Das and V.Ch. Venkata Rao for introducing me to the mathematical basis of the subject in their meetings.

I am also indebted to many friends who gave suggestions and helped me a lot in completing this work.

Final thanks are due to Mr. U.S. Misra for his patient and neat typing and Mr. B.K. Jain for his drawings.

IIT Kanpur

Krishna S.M. Medepalli

August, 1987

# CONTENTS

	<u>Page</u>
LIST OF FIGURES AND GRAPHS	III
NOMENCLATURE	V
ABSTRACT	VII
CHAPTER 1	
INTRODUCTION	1
Previous Works	3
Present Work	6
CHAPTER 2	
FORMULATION OF ADAPTIVE FINITE ELEMENTS	7
Basic Concepts of Grid Generation	7
Elliptic System	8
Poisson System	9
Attraction of Nodes to Coordinate Lines/Points	9
Adaptation Criteria	10
Weight Constant	12
Formulation for the FE Package	12
CHAPTER 3	
Test Problem-1	18
Conduction Problem	18
Verification	20
Adaptation	21
Grid Control Parameter	24
CHAPTER 4	
COMBUSTION PROBLEM	32
The Finite Element Equations	35
Channels Flow	36
Results	38
Uniform Grid Solutions	39
Adaptation	39
Conclusions	40
CHAPTER 5	
BOUNDARY LAYER PROBLEM	54
Numerical Solution	55
Boundary Conditions	56
Adaptation	56

CHAPTER 6

CONCLUSIONS  
Suggestions

APPENDIX A

APPENDIX B

REFERENCES

Page

60

62

63

64

65

## LIST OF FIGURES & GRAPHS

<u>Chapter 2</u>	<u>Page No.</u>
1 Grid line movement due to control functions	17
<u>Chapter 3 CONDUCTION IN A RECTANGULAR SLAB</u>	
1 Two dimensional steady heat conduction with uniform heat generation	25
2 Two dimensional steady heat conduction with non-uniform heat generation (uniform grid with 25 elements)	26
3 Isotherms for uniform 25 element grid	27
4 Grid after 4th adaptation	28
5 Isotherms for the adapted grid	29
6 Comparison of temperatures for the adapted and unadapted grids at chosen nodes	30
7 Comparison at chosen nodes	31
<u>Chapter 4 CHEMICALLY REACTING FLOW IN A CHANNEL</u>	
1. Uniform grid with 40 elements and boundary conditions	42
2a. $Y_1$ profile plotted for the 119 element grid (present work)	43
2b. $Y_1$ profile plot from Reference [9]	44
3a. u-velocity profile plotted for the 119 element grid (present work)	45
3b. u-velocity profile plot from Reference [9]	46
4a. Isotherms for the 119 element grid (present work)	47
4b. Isotherm plot from Reference [9]	48
5. $Y_1$ profile of 40 element adapted grid	49

6.	U-velocity profile of 40 element adaptive grid	50
7.	Isotherms of 40 element adaptive grid	51
8.	Grid structure after 6th adaptation	52
9.	Grid structure after 7th adaptation	53

## Chapter 5 BOUNDARY LAYER FLOW

1.	U-velocity profile at $x = 1.0$ $0 \leq y \leq 8.0$ in u-adapted case	58
2.	U-velocity profile at $x = 1.0$ $0 \leq y \leq 8.0$ in T-adapted case.	59

CORRIGENDUM:

1. See Table 5.2 and Table 5.3 for Fig. 5.2 and Fig. 5.3 respectively.
2. Fig. 4.9 is not included.
3. See Appendix C for computer timings.

## NOMENCLATURE

- $a$  = Half the width of the channel
- $B$  = Frequency factor in Arrhenious expression
- $C_p$  = Coefficient of specific heat at constant pressure
- $D$  = Binary diffusion coefficient
- $E$  = Activation energy per mole
- $f$  = Solution function used as basis for adaptation in Eqs. (2.2), (2.3)
- $g$  = Square of the determinant of Jacobian in Eq.2.7
- $h$  = Heat of formation per unit mass
- $i, j$  = Subscripts in FEM equation
- $K$  = Thermal conductivity
- $M$  = Molecular weight
- $n_e$  = Number of elements in the domain
- $P$  = Control function in Eq. 2.1
- $P_o$  = Ambient pressure
- $P$  = Pressure in Ch. 4
- $Q$  = Control function Ch. 2
- $Q'''$  = Heat generated per unit volume in Ch.3
- $q$  = Heat flux
- $R$  = Gas constant
- $S$  = Source term in Ch. 4
- $T$  = Temperature
- $u$  = X-direction velocity
- $v$  = Y-direction velocity
- $x$  = x-coordinate
- $y$  = y-coordinate
- $Y$  = Mass fraction



## Greek Symbols

- $\zeta$  = Local coordinate in an element
- $\eta$  = Local coordinate in an element
- $\xi$  = New x-coordinate
- $\eta$  = New y-coordinate
- $\rho$  = Density
- $\lambda$  = Constant used in Ch.4
- $\Omega$  = Bounded region of space
- $\Gamma$  = Boundary of the region bounded.

## Subscripts:

- $\alpha$  = Index for species
- T = Thermal

## ABSTRACT

A new adaptive finite element technique suitable for complex heat transfer and fluid flow problems has been developed and its edge over other existing adaptive grid techniques has been highlighted. The novel technique provides an automatic procedure of remeshing the finite element grid in such a way that high gradient regions receive due importance, which in turn results in an accurate solution of the physical problem considered.

The grid generation procedure is carried out in terms of body-fitted coordinates  $\xi$  and  $\eta$ . A poisson grid generation system is used for obtaining the  $\xi - \eta$  coordinate lines and the spacings between these lines in each direction are controlled with the help of suitable control functions. The gradient of the fastest varying solution variable have been used as the control function, with the sign of the second derivative governing the direction of grid movement.

The technique has been tested on three problems, namely, two dimensional steady heat conduction with non-uniform heat generation, reacting flow inside a rectangular channel and boundary layer flow over a flat plate with heat transfer. The results indicate that the present method works successfully for these types of complex fluid flow and heat transfer problems and that it is very effective in terms of accuracy and computational time as compared to unadapted grids.

## CHAPTER 1

### INTRODUCTION

Since the advent ~~and~~ digital computer numerical modelling of difficult engineering problems has become a viable alternative to expensive experimental modelling. Recent years have witnessed a ~~at~~tremendous increase in the speed of computation, with the result that problems whose solutions were thought to be cumbersome and unsolvable hitherto are now ~~now~~ solved efficiently. Several numerical techniques have been developed of which the finite difference and the finite element techniques have gained wide usage for finding the numerical solutions of engineering problems. The finite element method which provides the capability to develop very general and powerful packages is being accepted increasingly, in all disciplines including fluid mechanics and heat transfer. Both the methods require the division of the physical domain of the problem into a mesh with a finite number of intersecting lines which forms the computational grid. The present work is a complement to the above mentioned methods for finding the solutions of the transient, non-linear and other complex problems. The work deals with the distribution of the grid points in the domain in an effective manner such that the grid is suitable for the particular problem.

It has been noted by several authors [8] that when the grid is right most numerical solution methods work well. The numerical errors are reduced as the grid adapts to regions of large solution variation. Criteria such as orthogonality, smoothness and concentration of grid lines can be used for grid adaptation in order to get the most desirable grid structure. The adaptative grid is most effective when it is dynamically coupled with the physical solution (say temperature, velocity etc.) so that the solution and the grid are solved for together in a single continuous problem.

The various approaches for grid-adaptation that have been developed so far are essentially variational methods for the extremization of some solution property. Several considerations are involved here, some of which are sometimes conflicting. The points must concentrate and yet no region can be allowed to become devoid of points. The distribution also must retain a sufficient degree of smoothness, and the grid must not become too skewed, else the truncation error will be increased. This means that points must not, move independently, but rather each point must some how be coupled atleast to its neighbors. Also the grid points must not move too far or too fast, else oscillations may occur. Finally the solution error, or other driving measure, must be sensed, and there must be a mechanism for translating these into the motion of the grid. It should be noted that the use of an adaptive grid may not necessarily

increase the computer time even though more computations are necessary including those for obtaining the grids. However convergence properties of the solution may be improved and certainly fewer points will be required.

#### PREVIOUS WORKS:

A number of studies on adaptive grids are based on the point that the error can be reduced by distributing the grid points so that some positive weight function  $W(x)$  is equally distributed over the field. The variational methods or the other methods applied earlier are based on finite difference methods and selected different expressions for the weight function  $W(x)$  which essentially contains the first derivatives of the solution with respect to physical space. Moreover, the variational methods obtain the adapted grid, by solving the Euler-Lagrange equations obtained by the minimization of the integrals  $I_s$ ,  $I_o$  and  $I_w$  which represent smoothness, orthogonality and concentration of grid points respectively.

The adaptive grid procedure for the finite difference method has been pioneered by Dwyer and Sanders[1], Brackbill and Salzman[2], Rai and Anderson[3], Gnoffo[4] and Nakahashi, et al. [5]. Dwyer and Sanders have applied the smoothness approach to a two-dimensional curvilinear coordinate system with the grid points constrained to move along one family of fixed co-ordinate lines in proportion to the gradient of the dependent variable

$$d\xi \propto \left| \frac{\partial T}{\partial \xi} \right| ds$$

where  $\xi$  stands for the computational space,  $s$  for the physical space and  $T$  for the dependent variable of the original problem. The major difficulty with the method is the lack of control of grid skewness. The work by Gnoffo is based on spring analogy where springs connect adjacent mesh points and spring constants are a function of the gradient of some property and between the grid points. This work is extended by Nakahashi et.al. who considered a system of tension and torsional springs for multi-dimensional grids which control the spacings and skewness of the grid lines. The major drawback in the above mentioned methods is the finite difference basis on which they depend. This requires complex transformations of the equations from physical co-ordinates to computational co-ordinates and the numerical calculations of the derivatives is inaccurate. Also the numerical code may not be straight forward and certain parameters in the code are left to trial and error as seen in the work of Das[6]. Rai and Anderson proposed an attraction and repulsion criterion for grid point movement. This is accomplished by assigning to each grid an attraction proportional to the difference between the magnitude of some measure of error (or solution variation) and the average magnitude of this measure over all points. The use of higher derivatives in the error expressions was found to result in noisy measures and erratic point motion. This procedure does not exercise any control over either the smoothness or orthogonality and the grid, and therefore distortion is possible. There is

another approach, the chemical reaction analogy, which has not been studied thoroughly.

There are recent works which couple finite elements and adaptive grids. The moving finite elements of Miller is a dynamically-adaptive finite element grid method in which the grid point locations are made additional dependent ~~var~~ variables in a Galerkin formulation. The solution is expanded in piecewise linear functions, in terms of its values at the grid points and those of the grid point locations on each element. The residual is then required to be orthogonal to all the basis functions for both the solution and the grid. The grid point locations are thus obtained as part of the finite element solution. An internodal viscosity is introduced to penalize the relative motion between the grid points and an internodal repulsive force is introduced to maintain a minimum point separation. Both of these effects are strong but of short range. A small long range attractive force is also introduced to keep the nodes more equally spaced in the absence of solution gradients. Other recent works like that of Berger and Jameson [7] refine the existing grid at the locations where there is solution error. These are also automatic adaptations but the drawbacks of most of these are the usage of complicated numerical code and an increase in the computational time due to the increase in the number of nodes.

The present work includes a novel approach which uses finite elements and adapts the grid by solving an elliptic system of grid generation equations. The procedure can be applied to one, two and three dimensions with same ease. The method is tested on the following three problems:

- (i) Two-dimensional steady state heat conduction
- (ii) A steady chemically reacting flow in a rectangular channel
- (iii) The steady boundary layer flow over a flat plate with heat transfer.

In all the cases adaptation is applied on a coarse grid and the adapted grid results are compared with those of a coarse uniform grid and a fine uniform grid. Comparisons have also been made with exact analytical results where they are available. Thus the study brings forth the general applicability and the suitability of using the novel adaptive finite element method for the solution of complex heat transfer, fluid flow and combustion problems.



## CHAPTER 2

### FORMULATION OF THE ADAPTIVE FINITE ELEMENT PROCEDURE

#### BASIC CONCEPTS IN GRID GENERATION:

Grid generation techniques provide a systematic procedure for the placement of points within the solution domain so that a numerical grid with the desired control over grid spacing, orthogonality of grid lines and smoothness of grid line variation can be obtained. Some of these techniques exercise control over the node movement, whilst others generate grid lines using computational coordinates  $\xi$  and  $\eta$  whose intersection points provide the required grid. The attraction/repulsion method of grid adaptation [3] and the transfinite interpolation method [8] which involves an interpolation for the interior nodal points using the prescribed coordinate information for the boundary nodes, both result in algebraic grid generation equations. On the other hand, the methods which generate the computational coordinate lines  $\xi = \text{const}$  and  $\eta = \text{const}$ , invariably use partial differential equations of elliptic, parabolic or hyperbolic type. They aim to find the appropriate transformation from the physical coordinates  $x, y$  (for a 2-D problem) to the computational coordinates  $\xi$  and  $\eta$ . The solution of the physical problem itself may be carried out

either in terms of the physical coordinates or the computational coordinates, which ever is convenient.

In the present work, the elliptic grid generation system, which is one of the most popular techniques, has been employed in conjunction with the finite element method. If FEM is used for solving the physical problem also, then the computations can be conveniently performed in terms of the physical coordinates themselves, instead of transforming them in terms of the computational coordinates.

#### ELLIPTIC SYSTEM:

The adaptation of the grid can be viewed as the movement of lines/nodes due to the solution gradients i.e. the lines/nodes are moved towards high gradient regions and concentrated. Here use has been made of the properties of elliptic grid generation system. Some elliptic systems exhibit the extremum principles, i.e. the extrema of solutions cannot occur within the field. Such a feature is useful for grid generation since then maximum and minimum coordinates of a domain occur on the boundary. Another important property in regard to coordinate system generation is the inherent smoothness that prevails in the solution of elliptic systems. Furthermore, boundary slope discontinuities are not propagated into the field. The smoothness property and the extremum principles, allows grids to be generated for any configuration without overlap of grid lines.

## POISSON SYSTEM

Control of the coordinate line distribution in the field can be exercised by generalizing the elliptic generating system to a set of poisson equations:

$$\nabla^2 \xi^i = p^i \quad (i = 1, 2, 3) \quad (2.1)$$

in which control functions  $p^i$  can be fashioned to control the spacing and orientation of the coordinate lines. Here  $\xi^i$  are the computational coordinates. The extremum principles may be weakened or lost completely, with such a system, but the existence of an extremum principle is a sufficient, but not a necessary, condition for a one-to-one mapping, so that some latitude can be taken in the form of the control functions.

### ATTRACTION OF NODES TO COORDINATE LINES/POINTS

Let us consider the grid geometry shown in Fig.(2.1). For the poisson grid generation equation  $\nabla^2 \eta = Q$ , negative values of  $Q$  would tend to make the  $\eta$ -lines move in the direction of increasing  $\eta$ . While negative values of  $p$  in  $\nabla^2 \xi = p$  will cause  $\xi$ -lines to move in the direction of decreasing  $\xi$ . These effects are illustrated in Fig. (2.1) for an  $n$ -line boundary.

If the points on the boundary are free to move on it then the  $\xi$  -lines would move toward lines with lower values of  $\xi$  . On the other hand if the boundary nodes are fixed only the intersection angle will change at the boundary. Thus one may conclude that, in general, the negative values of the Laplacians of the dependent coordinates causes the lines on which that coordinate is constant, to move in the direction in which that coordinate decreases and vice versa.

#### ADAPTATION CRITERION:

As mentioned earlier the control functions can be manipulated so that the grid distribution can be done as desired. Here the first derivatives of the fastest varying solution variable are used as the control functions for adaptation. Therefore, the control functions P and Q can be written as

$$\begin{aligned} P &\sim \frac{\partial f}{\partial x} \\ Q &\sim \frac{\partial f}{\partial y} \end{aligned} \quad (2.2)$$

where x and y are the physical coordinates and f is the variable as the basis for adaptation. In the development of the present grid adaptation procedure, certain ideas from the technique of attraction of points/lines using control functions have been incorporated. The high gradient region in the original grid can be seen as a front to which lines or

points should converge. This is decided by the magnitude of the control function and the sign of it, while the magnitude gives the relative movement, the sign gives the direction to which the points/lines should move. When the magnitude of the gradient is increasing in the increasing x-direction the control functions should have +ve sign and vice versa.

The sign of the control function therefore, can be derived by considering the sign of the second derivative of the basis function. Here we can discuss <sup>five</sup> the cases in general.

- (i) first derivative +ve and its magnitude increases
- (ii) first derivative +ve and its magnitude decreases
- (iii) first derivative -ve and its magnitude increases
- (iv) first derivative -ve and its magnitude decreases
- (v) constant first derivative.

In all the above cases (except the last one) we can observe that

$$\frac{\partial f}{\partial x} \cdot \left| \frac{\partial^2 f}{\partial x^2} \right| / \frac{\partial^2 f}{\partial x^2}$$

controls both magnitude as well as the direction of node movement in the x-direction. Same is the case for the other direction y, in a two-dimensional case. Finally we add a weight 'W' to the control function for restricting th

extent of grid movement to reasonable values

$$\nabla^2 \xi + \frac{1}{W} \frac{\partial f}{\partial x} \cdot \left| \frac{\partial^2 f}{\partial x^2} \right| / \frac{\partial^2 f}{\partial x^2} = 0$$

$$\nabla^2 \eta + \frac{1}{W} \frac{\partial f}{\partial y} \left| \frac{\partial^2 f}{\partial y^2} \right| / \frac{\partial^2 f}{\partial y^2} = 0 \quad (2.3)$$

#### WEIGHT CONSTANT:

Here 'W' is a +ve number which may be large. The reason for taking large 'W' is that otherwise the control function on the right hand side may weaken or completely violate the extremum principle of the elliptic system. In order to avoid the predicament of grid points crossing the boundaries, the value of 'W' should be as large as possible. The value of 'W' however can be decided by the maximum gradient occurring in the domain for the solution variable used as the basis for adaptation. Another function of 'W' is to control the smoothness of grid. The large value of 'W' will not allow very much concentrated and rarified zones in the grid.

#### FORMULATION FOR THE FE PACKAGE:

The present scheme is based on a dynamically adaptive grid. So, the grid should be rearranged according to the variation of the solution in the physical problem, say temperature in a heat transfer problem. Either finite differences or finite elements can be used along with the grid

adaptation procedure for solving the physical problem. Here finite elements is preferred since it is versatile. Moreover it can be directly applied in the physical region unlike the finite differences where transformations to a rectangular computational domain are a must.

The only disadvantage with the scheme is that two equations are to be solved for the new coordinates. But this can be overlooked when we consider the solution accuracy and convergence (especially for non-linear problems). Also the computer time necessary for adaptation on a coarse grid may not be larger than that for a fine grid of same accuracy. This point has been repeatedly mentioned in the literature [8]. In the grid generation scheme the poisson system given by equations (2.3) is solved by the Galerkin technique or the weak formulation. Thus we have:

$$\sum_{i=1}^{ne} \iint_{\Omega} \rho_i \nabla^2 \xi^2 d\Omega + \iint_{\Omega} \rho_i \frac{1}{W} \left( \frac{\partial f}{\partial x} \right)_n \left| \frac{\partial^2 f}{\partial x^2} \right|_n / \left( \frac{\partial^2 f}{\partial x^2} \right)_n d\Omega = 0$$

$$\sum_{i=1}^{ne} \iint_{\Omega} \rho_i \nabla^2 \eta^2 d\Omega + \iint_{\Omega} \rho_i \frac{1}{W} \left( \frac{\partial f}{\partial y} \right)_n \left| \frac{\partial^2 f}{\partial y^2} \right|_n / \left( \frac{\partial^2 f}{\partial y^2} \right)_n d\Omega = 0 \quad (2.4)$$

where the subscript n denotes the value at a particular node n. The equations (2.4) can be integrated by parts to get,

$$\sum_1^{ne} \iint_{\Omega} \left( \frac{\partial \rho_i}{\partial x} \cdot \frac{\partial \xi}{\partial x} + \frac{\partial \rho_i}{\partial y} \frac{\partial \xi}{\partial y} \right) d\Omega = \sum_1^{ne} \iint_{\Omega} \rho_i \frac{1}{W} \left( \frac{\partial f}{\partial x} \right)_n \left| \frac{\partial^2 f}{\partial x^2} \right|_n$$

$$/ \left( \frac{\partial^2 f}{\partial x^2} \right)_n d\Omega$$

$$\sum_1^{ne} \iint_{\Omega} \left( \frac{\partial \rho_i}{\partial x} \frac{\partial \eta}{\partial x} + \frac{\partial \rho_i}{\partial y} \frac{\partial \eta}{\partial y} \right) d\Omega = \sum_1^{ne} \iint_{\Omega} \rho_i \frac{1}{W} \left( \frac{\partial f}{\partial y} \right)_n$$

$$\left| \frac{\partial^2 f}{\partial y^2} \right|_n / \left( \frac{\partial^2 f}{\partial y^2} \right)_n d\Omega \quad (2.5)$$

The line integrals arising from the integration by parts become zero when the boundary condition is ~~of~~ DIRICHLET type. The boundary conditions for grid generation are such that either the boundary conforming coordinate is specified or the normal derivative to the boundary is made equal to zero. This allows the grid points to move on boundaries also. So, ~~the~~ these boundary conditions are straight forward and can be easily incorporated into the grid generation scheme.

### Evaluating the Control Functions:

On the right hand side of equations ( 2.5 ) the first and second derivatives of the solution variable (which is used for adaptation) appear and these contributions need to be calculated at each node. In the evaluation of the elemental integrals, however, it is customary to use local coordinates  $\xi$  and  $\eta$  which facilitate numerical integration. An irregular



shaped element, for instance, is locally transformed into a square with  $\zeta$  and  $\eta$  as the local coordinates. All derivatives with respect to the global coordinates  $x$  and  $y$  need to be transformed in terms of the local coordinates  $\zeta$  and  $\eta$  and these transformations are performed according to the relations given by Thompson [8]. Therefore, the control functions can be expressed in terms of  $\zeta$  and  $\eta$  as :

$$\begin{aligned}
 f_x &= (\eta f_\zeta - \zeta f_\eta) / g \\
 f_y &= (-\zeta f_\zeta + \eta f_\eta) / g \\
 f_{xx} &= (\eta^2 f_{\zeta\zeta} - 2\zeta\eta f_{\zeta\eta} + \zeta^2 f_{\eta\eta}) / g \\
 &\quad + (\eta^2 \zeta_{\zeta\zeta} - 2\zeta\eta \zeta_{\zeta\eta} + \zeta^2 \zeta_{\eta\eta})(f_\zeta - \zeta f_\eta) \\
 &\quad + (\eta^2 \zeta_{\eta\eta} - 2\zeta\eta \zeta_{\eta\zeta} + \zeta^2 \zeta_{\zeta\zeta})(f_\eta - \eta f_\zeta) / g^{3/2} \\
 f_{yy} &= (\zeta^2 f_{\zeta\zeta} - 2\zeta\eta f_{\zeta\eta} + \eta^2 f_{\eta\eta}) / g \\
 &\quad + (\zeta^2 \eta_{\zeta\zeta} - 2\zeta\eta \eta_{\zeta\eta} + \eta^2 \eta_{\eta\eta})(f_\zeta - \zeta f_\eta) \\
 &\quad + (\zeta^2 \eta_{\eta\eta} - 2\zeta\eta \eta_{\eta\zeta} + \eta^2 \eta_{\zeta\zeta})(f_\eta - \eta f_\zeta) / g^{3/2}
 \end{aligned}
 \tag{2.6}$$

The terms such as  $x_{\xi}$ ,  $y_{\eta}$  etc. in the above relations are evaluated by knowing the transformation between  $x, y$  (global coordinates) and  $\xi, \eta$  (local coordinates). For isoparametric elements whose boundaries are expressed by the same order of curves as the order of interpolation within the element, it is possible to write :

$$x = \sum N_i(\xi, \eta) x_i$$

$$y = \sum N_i(\xi, \eta) y_i$$

and

$$\sqrt{g} = \begin{vmatrix} x_{\xi} & y_{\xi} \\ x_{\eta} & y_{\eta} \end{vmatrix} \quad (2.7)$$

where  $N_i$  are the interpolation functions for the solution variables.

After solving the two poisson equations (2.5a) and (2.5b), the computational coordinates  $\xi$  and  $\eta$  are obtained at all original grid points. Then  $\xi = \text{constant}$  lines and  $\eta = \text{const}$  lines are drawn by interpolating between the calculated nodal values of  $\xi$  and  $\eta$ . The intersection points between the  $\xi = \text{constant}$  and  $\eta = \text{constant}$  lines give the new grid points. In order to control the stability and convergence of the evolution of the grid, successive underrelaxation/overrelaxation technique is also employed. Details of the grid generation programme package are given in Appendix I.A.

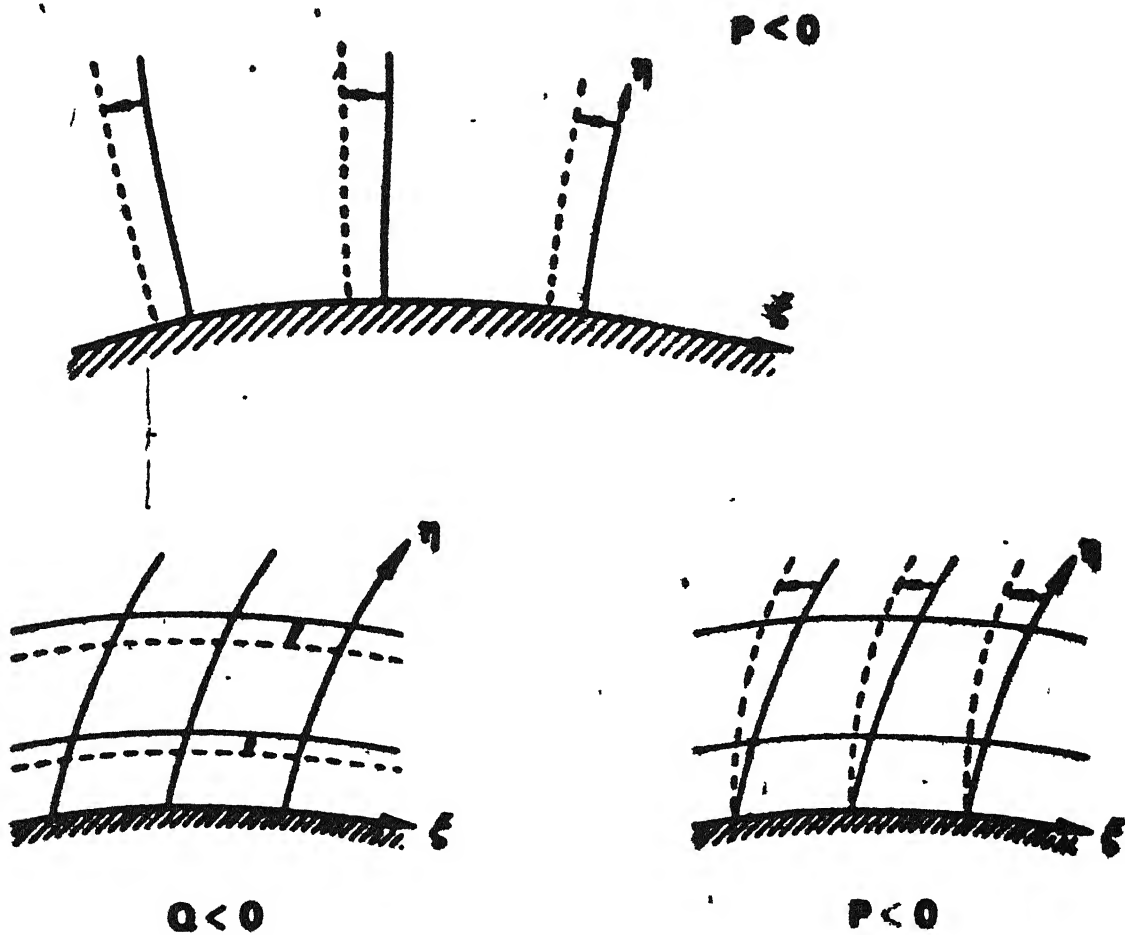


FIG. 2.1 : GRID LINE MOVEMENT DUE TO CONTROL FUNCTIONS

## CHAPTER 3

### TEST PROBLEM-1

The novel scheme of adaptive finite elements using a poisson system has been tested on three problems. Here it is intended to show the practicality of the method for heat transfer and fluid mechanics problems and the difficulties which arise in multi-dimensional cases. A FORTRAN package has been developed based on this technique for generating a 2-dimensional numerical grid which may be used to solve the heat transfer and fluid flow problems in conjunction with the FEM procedure or with any other suitable procedure. It is however, appropriate to point out here that if the problem is solved by FEM using 8-noded rectangular elements, elective and straight forward linking of the main program (of the problem) to the adaptive grid package is possible.

#### CONDUCTION PROBLEM:

The first test problem considered is that of steady state conduction in a rectangular slab. The equation governing the problem is given by,

$$k \nabla^2 T + Q''' = 0 \quad (3.1)$$

where  $T$  is the temperature and  $Q'''$  is the rate of heat generated per unit volume. In two dimensions the equation can be written as

$$\frac{\partial}{\partial x} \left( K \frac{\partial T}{\partial x} \right) + \frac{\partial}{\partial y} \left( k \frac{\partial T}{\partial y} \right) + Q^{**} = 0 \quad (3.2)$$

For finding the finite element solution of the above equation, the Galerkin's weighted residual approach is used, as follows:

$$\sum_1^{ne} \iint_{\Omega} \phi_1 \left[ \frac{\partial}{\partial x} \left( k \frac{\partial T}{\partial x} \right) + \frac{\partial}{\partial y} \left( k \frac{\partial T}{\partial y} \right) + Q^{**} \right] dx dy + \iint_{\Omega} \phi_1 Q^{**} dx dy = 0 \quad (3.3)$$

where  $\phi_1$  are the interpolating functions for the temperature. Integrating the above equation by parts and rearranging the terms we get,

$$\begin{aligned} \sum_1^{ne} \iint_{\Omega} k \left[ \frac{\partial \phi_1}{\partial x} \cdot \frac{\partial T}{\partial x} + \frac{\partial \phi_1}{\partial y} \cdot \frac{\partial T}{\partial y} \right] dx dy \\ = \sum_1^{ne} \iint_{\Omega} \phi_1 Q^{**} dx dy + \oint_{\Gamma_2} \phi_1 k \frac{\partial T}{\partial n} d\Gamma_2 \end{aligned} \quad (3.4)$$

where the last term indicates the line integral over the boundary ( $\Gamma_2$ ) of the solution domain ( $\Omega$ ) and is evaluated at the boundaries for Neumann or mixed boundary conditions. Expanding the variable  $T$  in terms of shape functions (or interpolation functions) the equation becomes

$$\begin{aligned} \sum_1^{ne} \iint_{\Omega} \left( \frac{\partial \phi_1}{\partial x} \frac{\partial \phi_1}{\partial x} + \frac{\partial \phi_1}{\partial y} \frac{\partial \phi_1}{\partial y} \right) dx dy T_j \\ = \sum_1^{ne} \iint_{\Omega} \phi_1 \frac{Q^{**}}{k} dx dy + \oint_{\Gamma_2} \phi_1 k \frac{\partial T}{\partial n} d\Gamma_2 \end{aligned}$$

I

In

In matrix form, for one element the left hand side and right-hand side contributions are respectively

$$\begin{bmatrix} a_{11} & a_{12} & \dots & a_{18} \\ a_{21} & a_{22} & \dots & a_{28} \\ \vdots & \vdots & \ddots & \vdots \\ a_{81} & a_{82} & \dots & a_{88} \end{bmatrix} \quad \text{and} \quad \begin{Bmatrix} b_1 \\ b_2 \\ \vdots \\ b_8 \end{Bmatrix}$$

where,

$$a_{ij} = \iint_{\Omega} \left( \frac{\partial \phi_i}{\partial x} \cdot \frac{\partial \phi_j}{\partial x} + \frac{\partial \phi_i}{\partial y} \cdot \frac{\partial \phi_j}{\partial y} \right) dx dy \quad (3.6)$$

$$b_i = \iint_{\Omega} \phi_i \frac{Q'''_0}{k} dx dy + \int_{\Gamma_2} \phi_i k \frac{\partial T}{\partial n} d\Gamma_2 \quad (3.7)$$

For all the elements similar LHS and RHS contributions arise which can be assembled to form a set of algebraic equations for all the nodal variables. The final solution can be obtained after substituting the Dirichlet condition (if there is any) by matrix inversion of the nodal equations.

#### VERIFICATION:

The program developed for conduction has been tested for correctness with the help of a known solution. Steady state heat conduction in a rectangular slab is considered with

the following data, as shown in Fig. (3.1):

$$\begin{aligned}
 Q'''/K &= 1.0 \\
 q_{x=0} &= 0 \\
 q_{y=0} &= 0 \\
 T_{x=1} &= 0 \\
 T_{y=1} &= 0
 \end{aligned} \tag{3.8}$$

Results are tabulated for 4 elements and 16 elements (both 8-noded rectangular) along with the series solution. The 16 element solution and series solution are almost identical. See Table 3.1.

#### ADAPTATION:

In the present problem (Fig. 3.2) to highlight the effects of grid adaptation, the heat generation term is taken as an exponential function of co-ordinates so that high temperature gradients occur in certain regions. It is given by,

$$Q''' = Q_0''' e^{-\rho\{(x-1)^2 + (y-1)^2\}} \tag{3.9}$$

The boundary conditions are:

$$\begin{aligned}
 q_{y=0} &= 0 \\
 q_{x=0} &= 1.0 \\
 T_{y=2} &= T_0 \\
 k \frac{\partial T}{\partial x} \Big|_{x=2} &= h(T - T_{amb})
 \end{aligned} \tag{3.10}$$

The property values and other constants in the equations are taken as follows:

TABLE 3.1

$y$	$T(o, y)$ 4 elements	$T(o, y)$ 164 elements	$T(o, y)$ series solution
0.0	0.2941	0.2946	0.2947
0.25	0.2790	0.2783	0.2789
0.50	0.2292	0.2293	0.2293
0.75	0.1396	0.1397	0.1397
1.00	0.0000	0.0000	0.0000



$$\begin{aligned}
 Q_0'' &= 10^4 \\
 h &= 10 \\
 T_{\text{amb}} &= 10 \\
 T_0 &= 100 \\
 k &= 200.0 \\
 P &= 10
 \end{aligned}
 \tag{3.11}$$

The problem is solved for 25 elements (96 nodes) and for 100 elements (347 nodes), using a uniform mesh. The adaptation is carried out on a coarse grid (25 elements). For adaptation the connectivity,  $x$  and  $y$  co-ordinates of the nodes and the solution obtained by coarse grid are required. As mentioned in Chapter 2 the new co-ordinates  $\xi$  and  $\eta$  should be boundary conforming. The  $\xi$  values at  $x = 0$  and  $x = x_{\text{max}}$  lines are specified. Similarly  $\eta$  values on  $y = 0$  and  $y = y_{\text{max}}$  are specified. The points are free to move on the boundaries also. The specified  $\xi$  and  $\eta$  become Dirichlet boundary conditions for the system of grid generation equations (Equation 2.1). After each adaptation the temperatures in the slab are found by the conduction program.

Figure (3.2) to Figure (3.5) show the evolution of the grid from the initial uniform mesh to the final adapted mesh. The regions of high gradients can be clearly observed from these figures. The grid adaptation is performed four times and the final results of the temperature variation is presented in Figure (3.6) and Figure (3.7) for different nodes which lie on a chosen curve. For comparison the coarse grid

adaptive grid and fine grid results for corresponding points are plotted on the same graph, after interpolating the coarse grid and fine grid solutions. The figures show that the adapted grid solution falls between the coarse grid solution and fine grid solution. The nearness of the solution of adapted grid to that of fine grid is apparent after repeated adaptations.

#### GRID CONTROL PARAMETER:

Definitely there should be some control over the grid point movement so as to adhere to the principles of smoothness and orthogonality at the boundaries of the grid. Truly much study has not been done on this aspect. But in general the high value of 'W' (+ve) in Eqn. (2.3) gives stiff resistance to grid point movement. This is due to the reason that the high value of 'W' makes the right hand side less and in turn the Laplacian properties are retained. For initial guess the value may be of the order of absolute maximum of the solution gradient. The value of 'W' is increased for each successive adaptation by a small amount so that smoothness trouble may not arise. An important point that needs to be mentioned is that the new grid points may shoot out of the boundaries if the value of W is very small when compared to the gradient values. In the current problem the value chosen for W is 50.0 and it is increased 1.25 times after each adaptation. From the above discussion it is clear that the parameter 'W' is problem dependent and varies according to the maximum gradient (abs. value) of the solution.

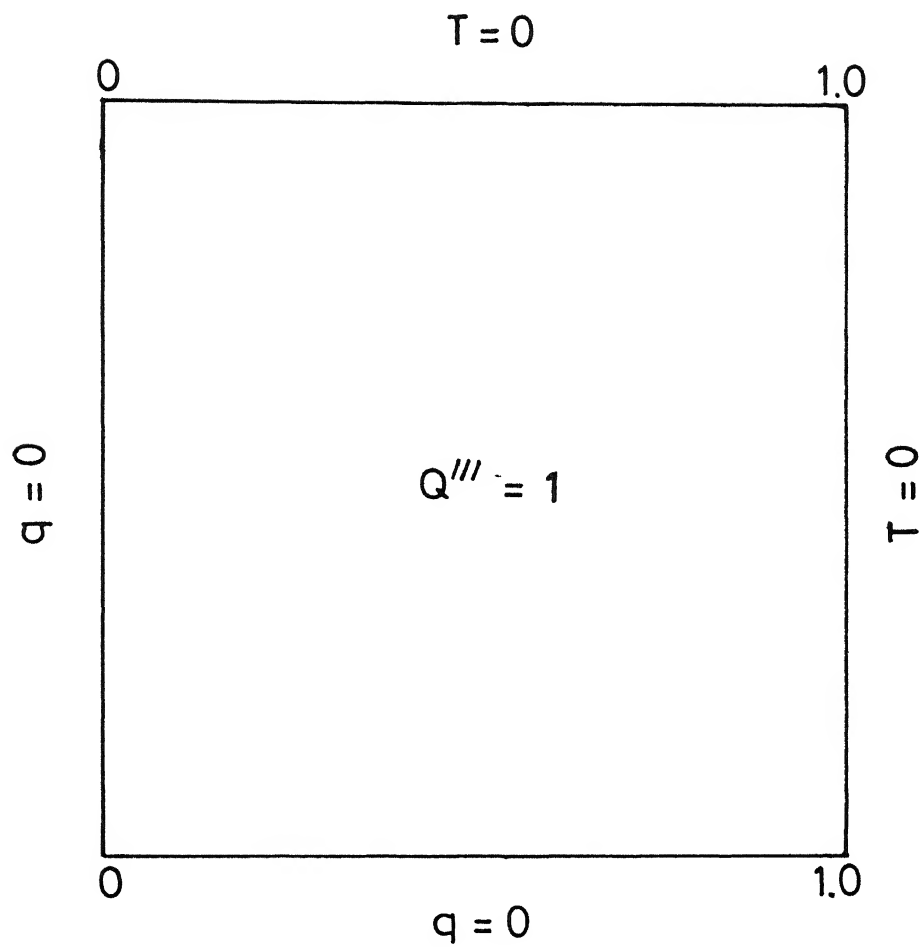


Fig. 3.1 Two dimensional steady heat conduction with uniform heat generation.

$$T = 100$$


$$h(T - T_{amb})$$

$$\theta = 0$$

$$Q = 0$$

Fig 3 2 CONDUCTION WITH NON-UNIFORM HEAT GENERATION

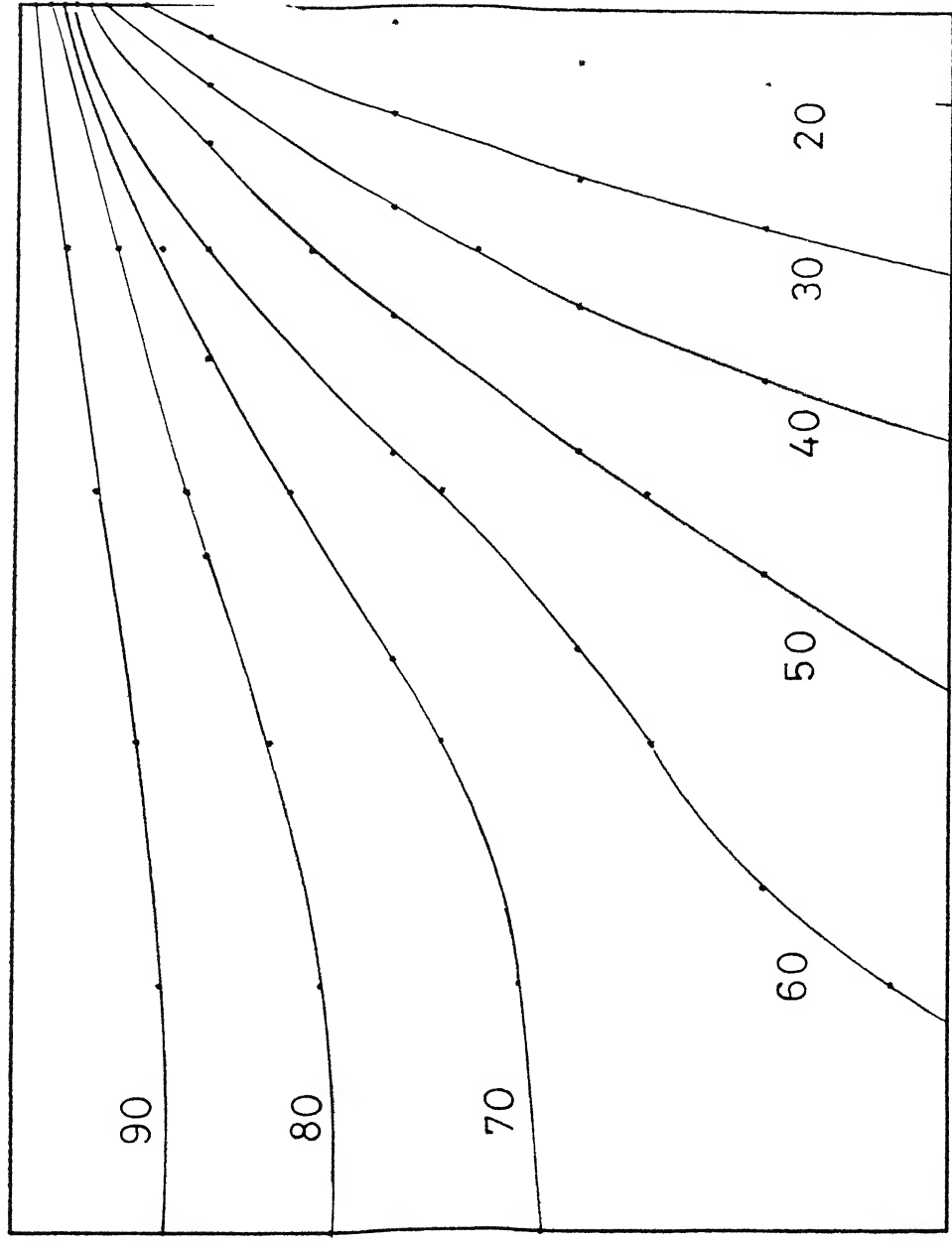


FIG3.3 ISOTHERMS FOR UNIFORM 25 ELEMENT GRID

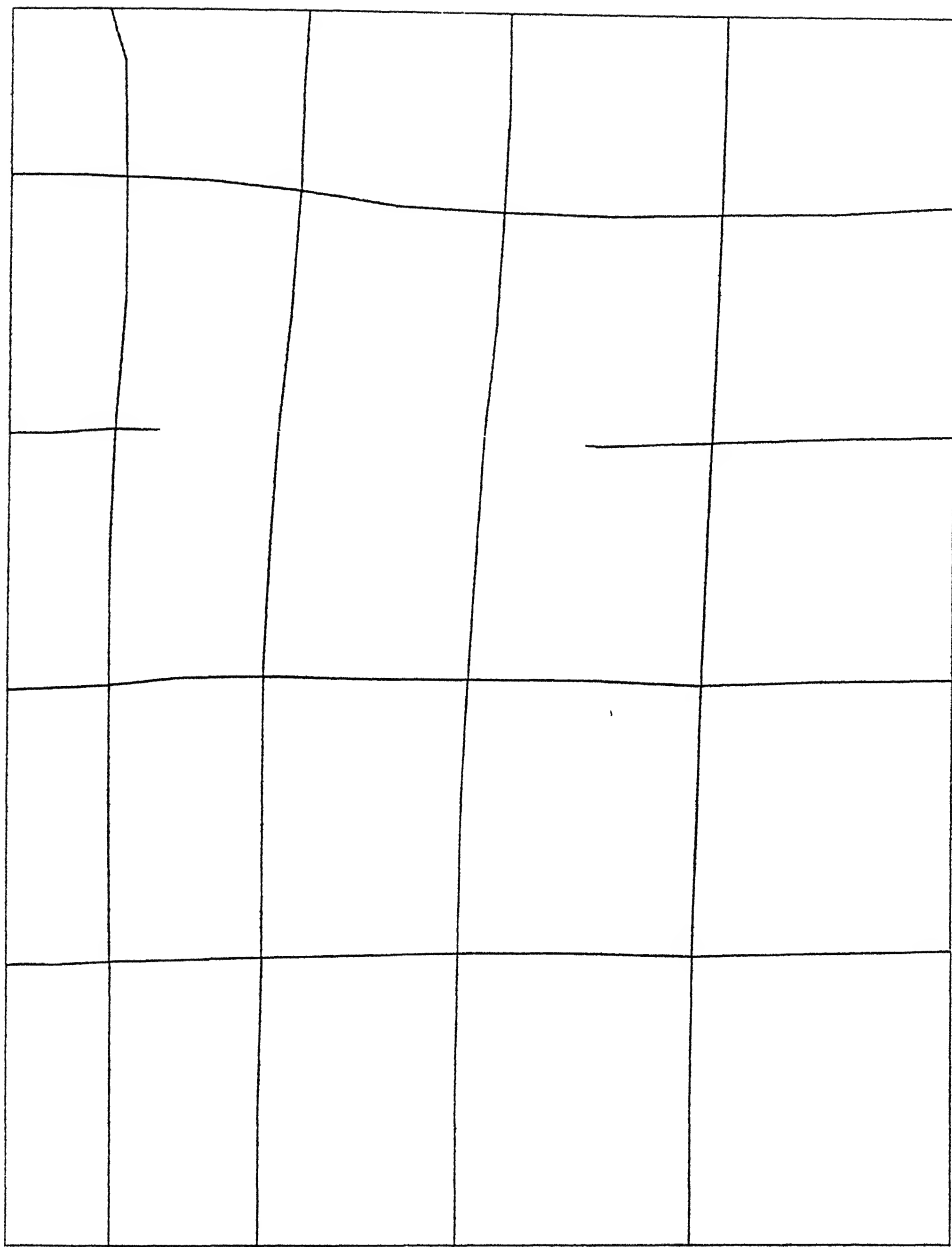


FIG3 4 GRID AFTER 4TH ADAPTATION

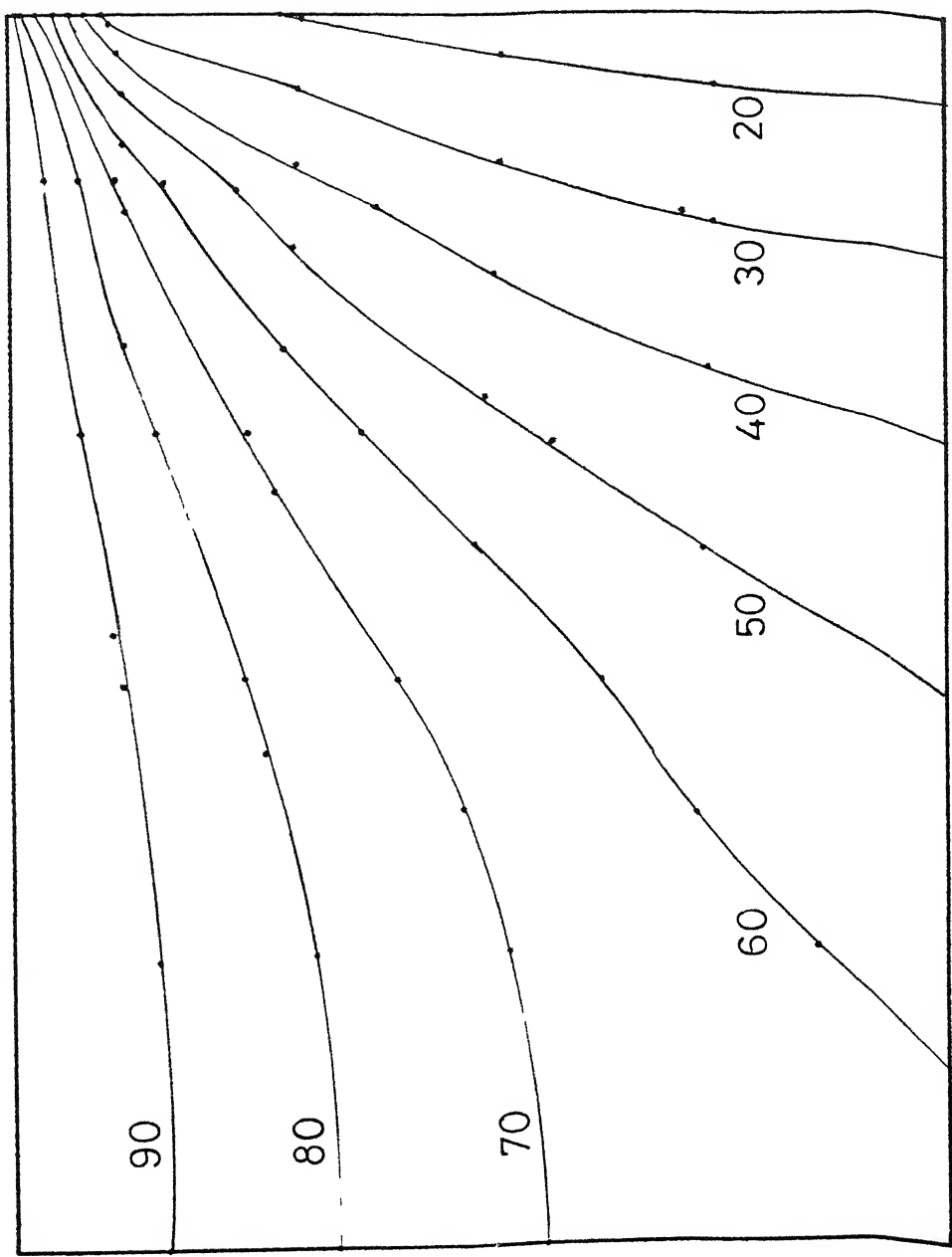


FIG3.5 ISOTHERMS FOR ADAPTED 25 ELEMENT GRID .

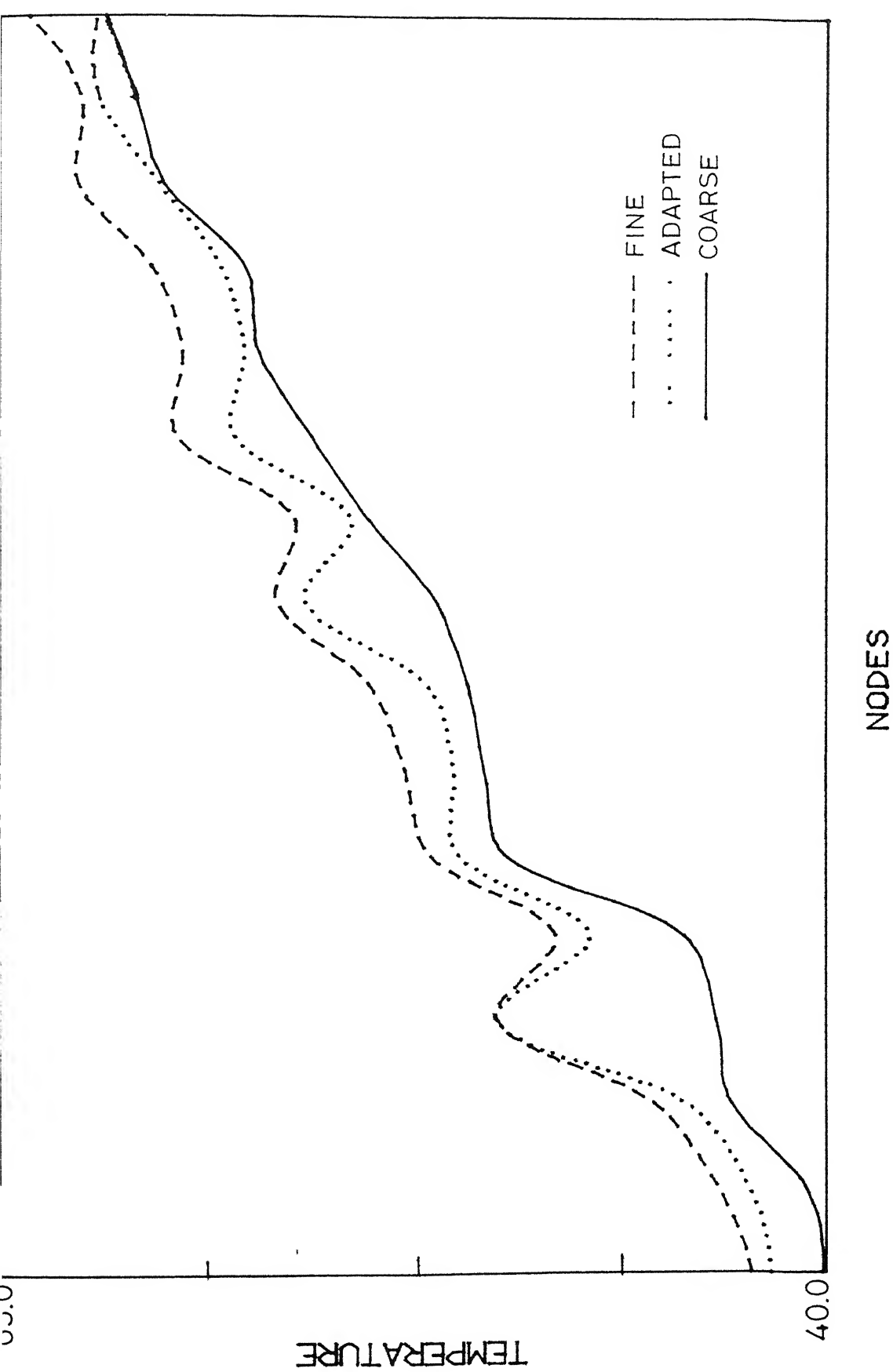


FIG3.6 COMPARISON OF TEMPERATURES FOR THE ADAPTED  
AND UNADAPTED GRIDS AT CHOSEN NODES



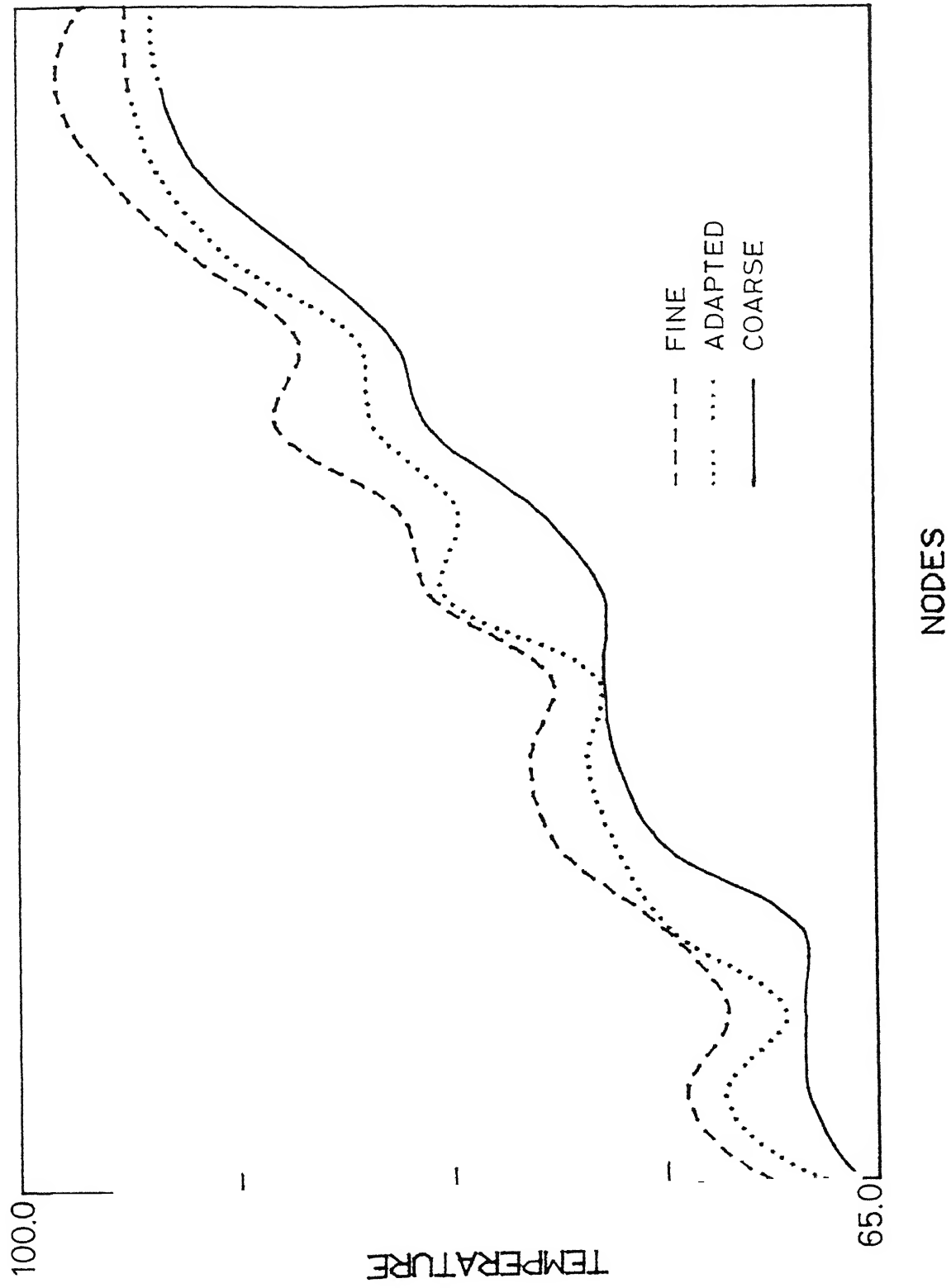


FIG3.7 COMPARISON OF TEMPERATURES FOR THE ADAPTED AND UNADAPTED GRIDS AT CHOSEN NODES

## CHAPTER 4

### COMBUSTION PROBLEM

The second problem considered for demonstrating the capabilities of the proposed adaptive finite element technique is the laminar flow with chemical reaction in a rectangular channel [9]. This is a typical combustion problem which is highly non-linear with severe convergence difficulties.

Combustion problems usually are characterized by fast chemical reaction processes which lead to high temperature and concentration gradients in certain regions. The grid for numerical modelling must be suitably formed to capture these high gradients failing which severe inaccuracies in the final solution may occur. The location and magnitude of the high temperature and concentration gradients are not available a priori and therefore, adaptive grid procedure is a very effective way to tackle such problems.

The present physical problem is treated as a steady two-dimensional flow of gas in which transport of three chemical species - a fuel, an oxidant and a product occur. The reaction between the oxidant and fuel releases heat and this heat is also transported by the fluid flow. The local changes in temperature and species concentration modify the local density and hence the flow pattern itself. Thus it is essential

to solve the coupled equations of mass, momentum, energy and species to obtain velocities, pressure, temperature and concentrations.

The governing equations are taken as follows:

X-mom:

$$\rho u \frac{\partial u}{\partial x} + \rho v \frac{\partial u}{\partial y} + \frac{\partial p}{\partial x} - 2 \frac{\partial}{\partial x} (\mu \frac{\partial u}{\partial x}) - \frac{\partial}{\partial y} \mu (\frac{\partial u}{\partial y} + \frac{\partial v}{\partial x}) = 0 \quad (4.1)$$

Y-mom:

$$\rho u \frac{\partial v}{\partial x} + \rho v \frac{\partial v}{\partial y} + \frac{\partial p}{\partial y} - 2 \frac{\partial}{\partial y} (\mu \frac{\partial v}{\partial y}) - \frac{\partial}{\partial x} \mu (\frac{\partial u}{\partial y} + \frac{\partial v}{\partial x}) = 0 \quad (4.2)$$

Continuity:

$$\frac{\partial}{\partial x} (\rho u) + \frac{\partial}{\partial y} (\rho v) = 0 \quad (4.3)$$

Energy:

$$\rho u \frac{\partial C_p T}{\partial x} + \rho v \frac{\partial C_p T}{\partial y} - \frac{\partial}{\partial x} \left( \frac{k}{C_p} \frac{\partial C_p T}{\partial x} \right) - \frac{\partial}{\partial y} \left( \frac{k}{C_p} \frac{\partial C_p T}{\partial y} \right) = S_T \quad (4.4)$$

Species:

$$\rho u \frac{\partial Y_\alpha}{\partial x} + \rho v \frac{\partial Y_\alpha}{\partial y} - \frac{\partial}{\partial x} \left( \rho D \frac{\partial Y_\alpha}{\partial x} \right) - \frac{\partial}{\partial y} \left( \rho D \frac{\partial Y_\alpha}{\partial y} \right) = S_\alpha \quad (4.5)$$

$\alpha = 1, 2$

The important assumptions involved in obtaining the above equations are:

- (1) All pairs of species have same value of diffusion coefficient.
- (2) Body forces are absent.
- (3) Pressure work and viscous dissipation are negligible.
- (4) All properties except density are constants.

As for the third species one obtains from

$$Y_1 + Y_2 + Y_3 = 1 \quad (4.6)$$

$$S_1 + S_2 + S_3 = 0 \quad (4.7)$$

where the symbols  $x$ ,  $y$ ,  $u$ ,  $v$ ,  $T$ ,  $Y_\infty$ ,  $S$ ,  $k$ ,  $p$  and  $C_p$  stand for the usual notation and  $D$  stands for the binary diffusion coefficient.

Finally closure for the above set of equations requires the specification of the mass and heat sources from the rate of chemical reaction and the thermodynamic equations of state, which relates density, pressure, temperature and the mass fractions.

From the perfect gas law for ideal mixtures

$$S = \left( \frac{p_0 + p}{R_g T} \right) \left[ \frac{Y_1}{M_1} + \frac{Y_2}{M_2} + \frac{Y_3}{M_3} \right]^{-1} \quad (4.8)$$

Rate of production of species :

$$S_{\alpha} = \gamma_{\alpha} M_{\alpha} B e^{-E/RT} \left( \frac{Y_1}{M_1} \right) \left( \frac{Y_2}{M_2} \right) \quad (4.9)$$

$\alpha = 1, 2$

$$S_T = - \sum_{n=1}^3 h_n S_n \quad (4.10)$$

As far as the boundary conditions are concerned on solid wall boundaries the velocities have to be set to zero but the heat and mass fraction variables may have either specified fluxes or specified values. On axes of symmetry normal velocities and normal derivatives of other variables have to be set to zero. The inlet profiles of  $u$ ,  $v$ ,  $T$  and  $Y_{\alpha}$  are specified. At the outlet the velocity, temperature and concentration profiles are taken to be fully developed.

#### THE FINITE ELEMENT EQUATIONS:

The program incorporated isoparametric elements consisting of 8-noded quadrilaterals having quadratic variation. The pressure is represented by linear functions because of the lower order derivatives of pressure and the remaining variables,  $u$ ,  $v$ ,  $T$ ,  $Y$  and are represented by quadratic functions. The Galerkin technique is applied to get the finite element equations. For example the species equation (4.5) can be integrated as follows:

$$\begin{aligned}
& \sum_i \int_{\Omega} \phi_i \left( S u \frac{\partial Y_{\alpha}}{\partial x} + S v \frac{\partial Y_{\alpha}}{\partial y} \right) dx dy \\
& + \int_{\Omega} \frac{\partial \phi_i}{\partial x} \int_{\Gamma_1} D \frac{\partial Y_{\alpha}}{\partial x} d\Omega + \frac{\partial \phi_i}{\partial y} \int_{\Gamma_1} D \frac{\partial Y_{\alpha}}{\partial y} d\Omega \\
& - \int_{\Gamma_2} \phi_i \int_{\Omega} D \frac{\partial Y_{\alpha}}{\partial n} d\Omega - \int_{\Omega} \phi_i S_{\alpha} d\Omega = 0 \\
& i = 1, 2, \dots, 8 \quad (4.11)
\end{aligned}$$

where  $\phi_i$  are the shape functions for quadratic variation and  $\Omega$  is the solution domain.

On the part of the boundary  $\Gamma_1$  the variable  $Y_{\alpha}$  is specified and on the boundary  $\Gamma_2$  the derivative  $\partial Y_{\alpha} / \partial n$  is specified.

The other equations can also be integrated exactly in a similar way. The continuity equation is handled differently as observed in other works in literature [9]. This is integrated with respect to linear weighting functions as follows:

$$\int_{\Omega} \psi_i \left( \frac{\partial (S u)}{\partial x} + \frac{\partial}{\partial y} (S v) \right) d\Omega = 0 \quad i = 1 \dots 4 \quad (4.12)$$

where  $\psi_i$  are the shape functions for linear variation.

#### CHANNEL FLOW:

Two reacting species flow along a two-dimensional channel and the heat released disturbs the flow which at the inlet had been fully developed. One of the species,  $\alpha = 1$  say is assumed to be very dilute compared to the other, so that the

reaction may be regarded as being effectively of first order and species equations other than that of  $Y_1$  need not be considered.

The source term for the mass fraction of the dilute species, appearing in equation 4.5 is then taken to be

$$S_1 = -\lambda Y_1 \quad (4.13)$$

which is independent of the temperature. For the equation of state we assume the form

$$g = 300/T \quad (4.14)$$

corresponding to uniform chemical composition. For the case of no heat release ( $h_{\infty} = 0$ ), the flow remains fully developed and the equation for  $Y_1$  need only be solved.

With the origin of the rectangular co-ordinates being at the midpoint of the inlet, the boundary conditions for the cases of no heat release and heat release are taken as follows (Figure 4.1).

$$(1) \text{ Inlet } (x = 0; -a \leq y \leq a)$$

$$u = u_0 (1 - y^2/a^2)$$

$$v = 0$$

$$T = 300$$

$$Y_1 = Y_1^{IN}$$

(2) TOP and bottom walls ( $0 \leq x \leq 0.5$ ,  $y = \pm a$ )

$$u = v = \frac{\partial Y_1}{\partial y} = 0$$

$$T = 300$$

(3) Outlet ( $x = 0.5$ ;  $-a \leq y \leq a$ )

$$\frac{\partial u}{\partial x} = v = p = \frac{\partial T}{\partial x} = \frac{\partial Y_1}{\partial x} = 0 \quad (4.15)$$

The following values of the constants are taken:

$$D = 10^{-4} \text{ m}^2/\text{s}$$

$$K = 0.1 \text{ W/m/K}$$

$$C_p = 1000 \text{ J/kg/K}$$

$$h_3 = 5 \times 10^5 \text{ J/mol}$$

$$h_1 = h_2 = 0$$

$$\mu = 1.8 \times 10^{-5} \text{ kg (m/s)}$$

$$\lambda = 1$$

$$a = 0.05 \text{ m}$$

$$\text{Length} = 0.5 \text{ m}$$

$$\text{Width} = 0.1 \text{ m} \quad (4.16)$$

#### RESULTS:

Uniform <sup>grid</sup> solutions for the above mentioned problem is obtained in order to check the correctness of the program code of the present study by comparing with the available results of [9] who have also solved this problem using a uniform FEM mesh.



## UNIFORM GRID SOLUTIONS:

The domain is divided into uniform 8-noded rectangular elements with 17 elements in x-direction and 7-elements in y-direction. The total number of nodes is 406 and the total degrees of freedom are 1768. For numerical integration 9-point gaussian quadrature has been used. Picard's iteration procedure is used 7 times to secure convergence.

In the case of flow with no heat release the convergence is obtained in the first iteration itself since  $u$ ,  $v$ , and  $T$  are constant. The profiles of mass fraction  $Y_1$  at different sections has been presented in Fig. (2.a). These can be compared with the profiles given in [ 9 ], which have been reproduced in Fig.(2.b.)

In the case of flow with heat release the  $u$ -velocity at different sections is plotted in Figure (4.3a). These can be compared with the profiles given in [ 9 ] which have been reproduced in Fig. (4.3b). The profiles of mass fraction and velocity show good coincidence with that of [ 9 ].

The isotherms for the heat release case are plotted in Fig.(4.4a) which are compared with the isotherm plot of [ 9 ], reproduced here in Fig.(4.4b)

## ADAPTATION:

The adaptation is carried out on a smaller grid and 40 elements (10x4) and 149 nodes with 651 degrees of freedom.

Gradients in species have been chosen as the basis, for adaptation when there is no heat release since the problem is isothermal. This choice for adaptation will smooth the discrepancies arising due to the species variation. For the situation with heat release adaptation is carried on the basis of temperature because of the rapid variations in temperature which disturb the density and consequently, the velocities and species. Totally six iterations are carried out for obtaining the required result. The profiles of species and velocities are given in Fig. (4.5) and Fig. (4.6). The isotherms are plotted in Fig. (4.7).

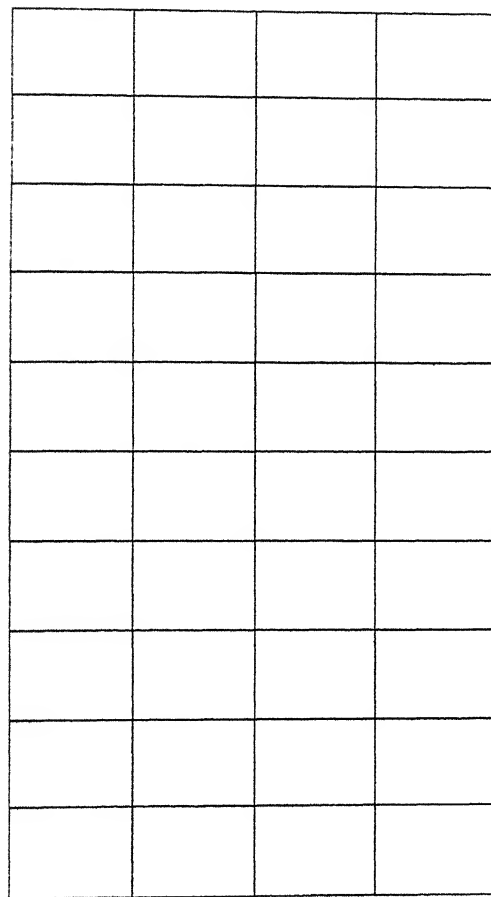
The adapted grides are shown in Fig. (4.8) and Fig. (4.9). The adaptation not only reduces the computational time but also gives the idea of the variations in the field variables. A remarkable feature in the adaptation of combustion problems is that the grid itself shows the location of heat release and flame. This can be observed in Fig. (4.9).

#### CONCLUSIONS:

- (1) For starting the iterative procedure for the heat release case the solution from the no heat release case is taken as the initial guess. This ensures fast convergence.

- (2) As far as possible the temperature should be under-relaxed so that the equations are not perturbed strongly.
- (3) The choice of the weight 'W' which controls the rate of grid movement between two successive iterations, depends on the maximum derivative of the variable used as the basis for adaptation. Larger the derivative, larger the value of 'W' which will give a stable numerical solution.

$$U=V=0 \quad T=300, \quad DY1/DY=0$$



$$U=UIN \quad V=0 \\ T=300, \quad Y1=Y1IN$$

$$DU/DX=0, \quad V=P=0$$

$$DT/DX=0, \quad DY1/DX=0$$

$$U=V=0, \quad T=300, \quad DY1/DY=0$$

FIG4 1 UNIFORM GRID WITH 40 ELEMENTS AND BOUNDARY CONDITIONS

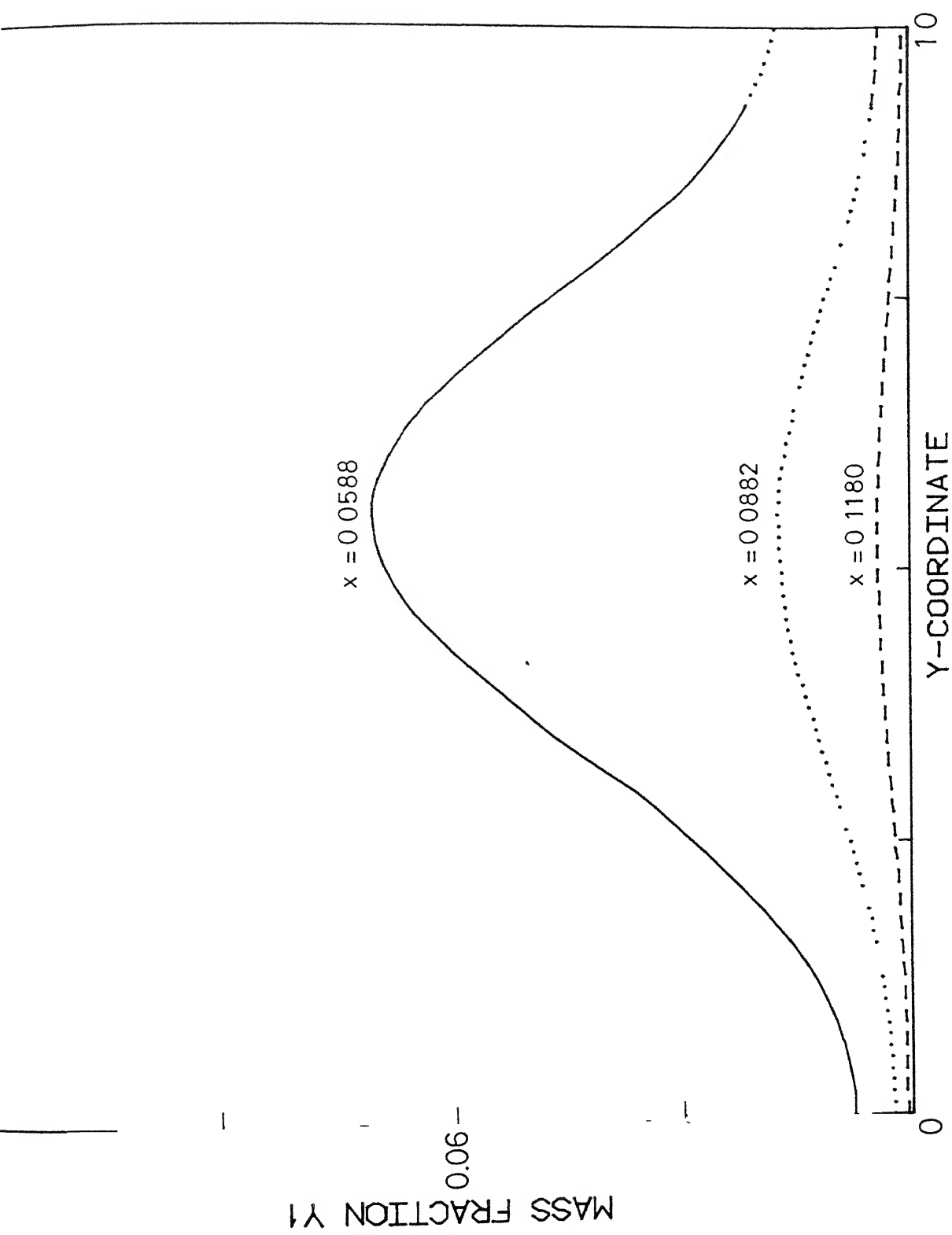


FIG4 2A Y1 PROFILE PLOTTED FOR 119 ELEMENT GRID

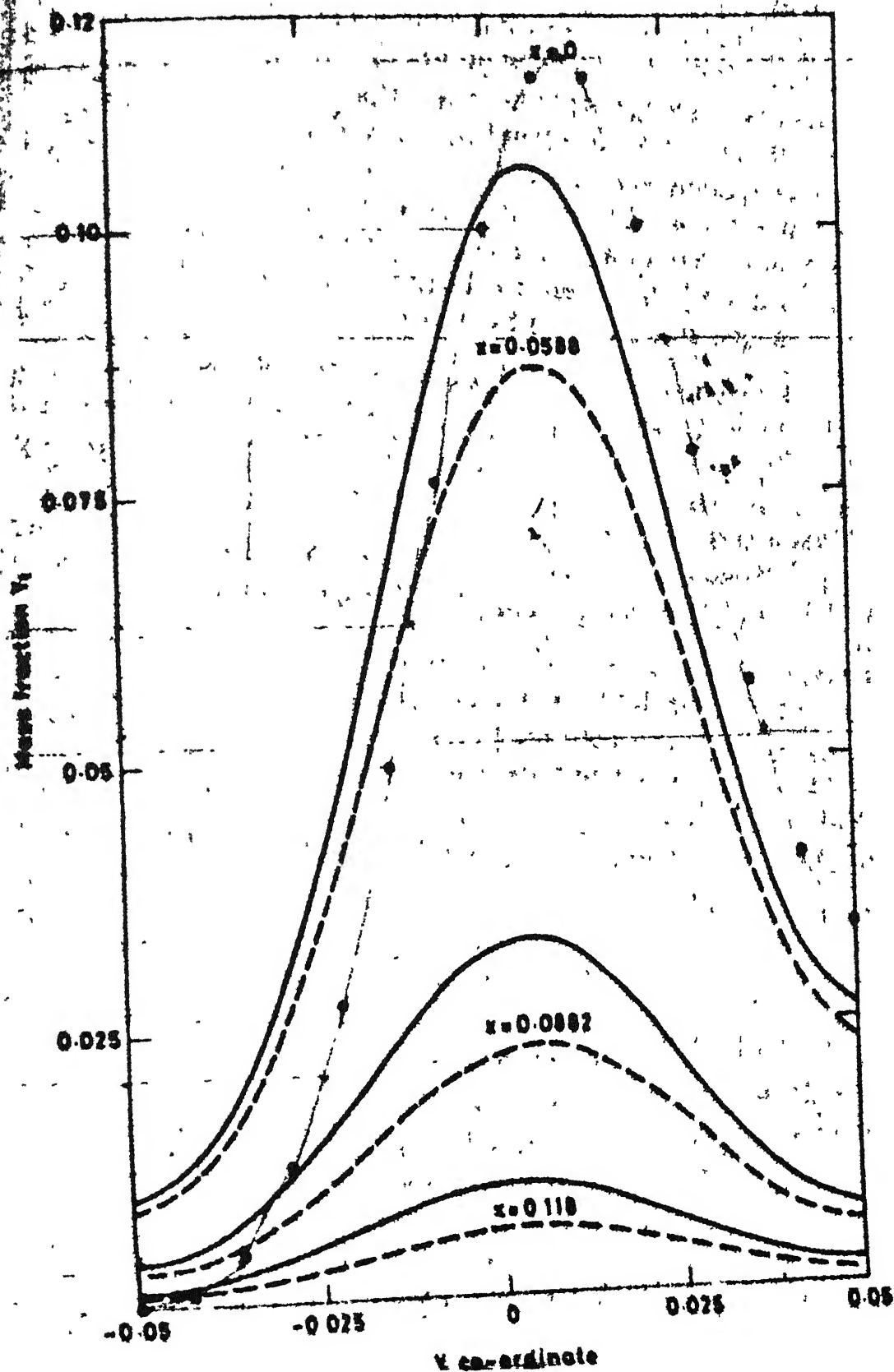


FIG. 4.2B :  $Y_1$  PROFILE FROM REFERENCE [9]  
BROKEN LINES FOR THE CASE OF HEAT RELEASE

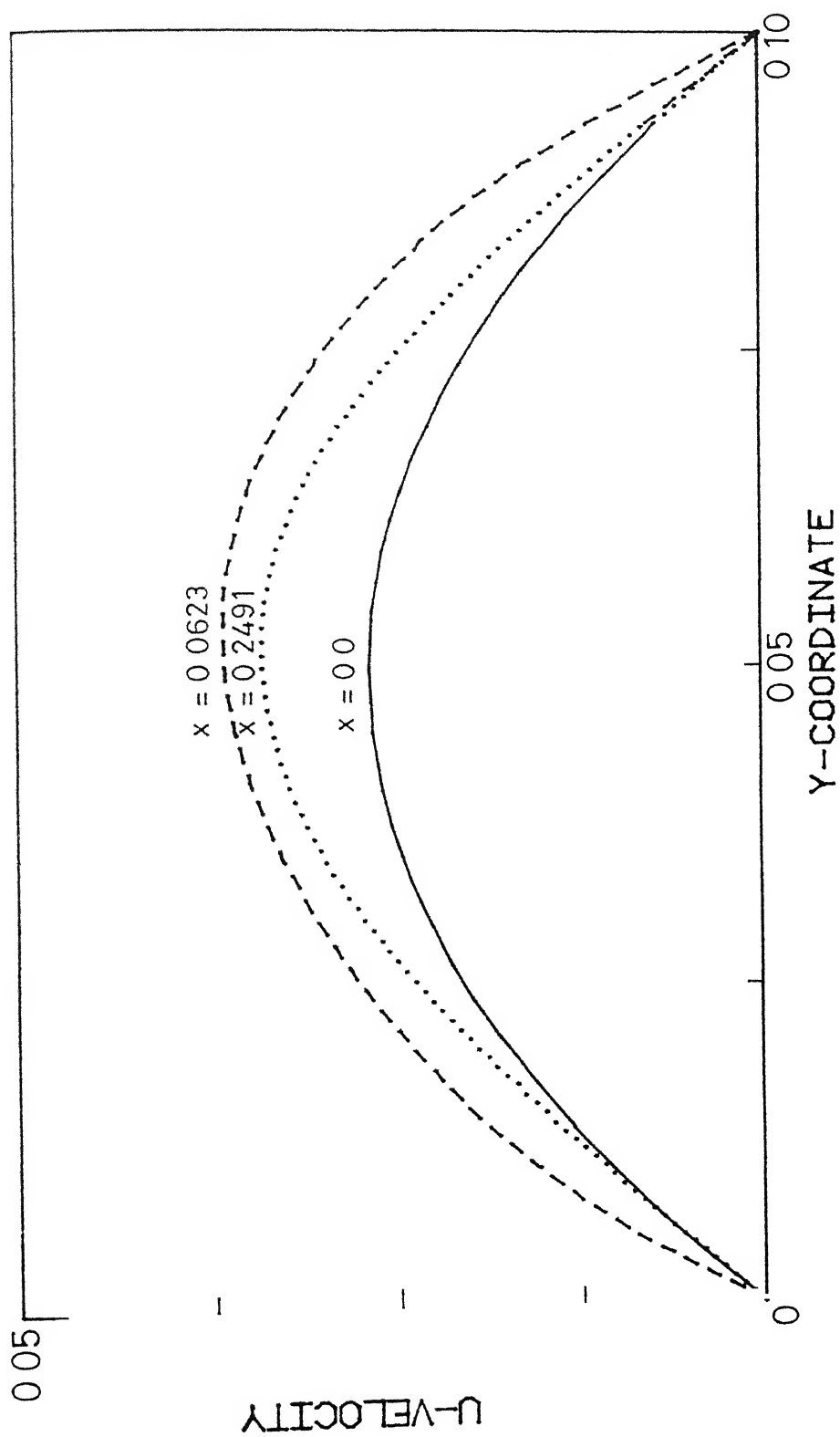


FIG4.3A U-VELOCITY PROFILE PLOTTED FOR 119 ELEMENT GRID

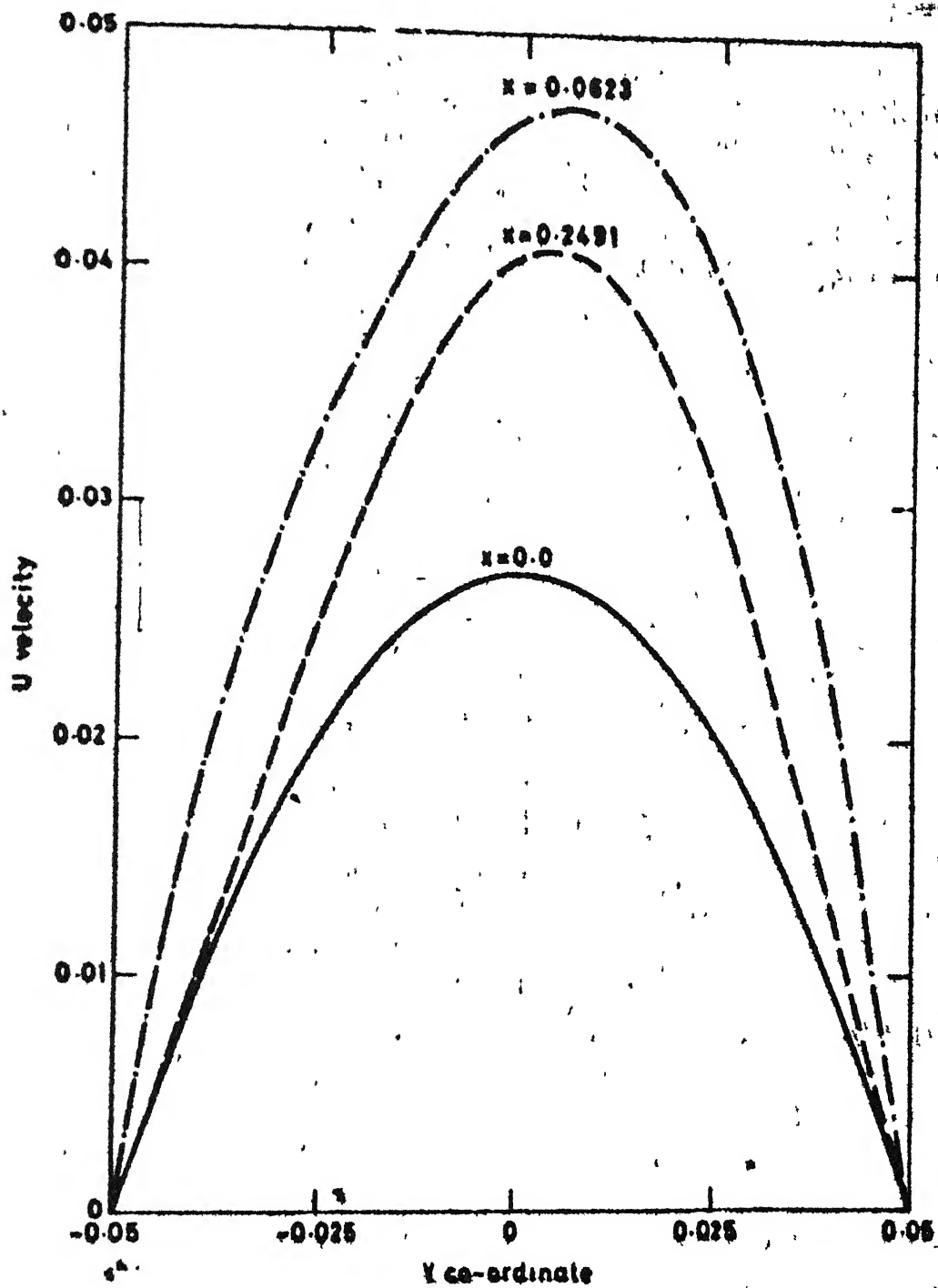


FIG. 4.3B : U-VELOCITY PROFILE PLOT FROM REFERENCE [9]



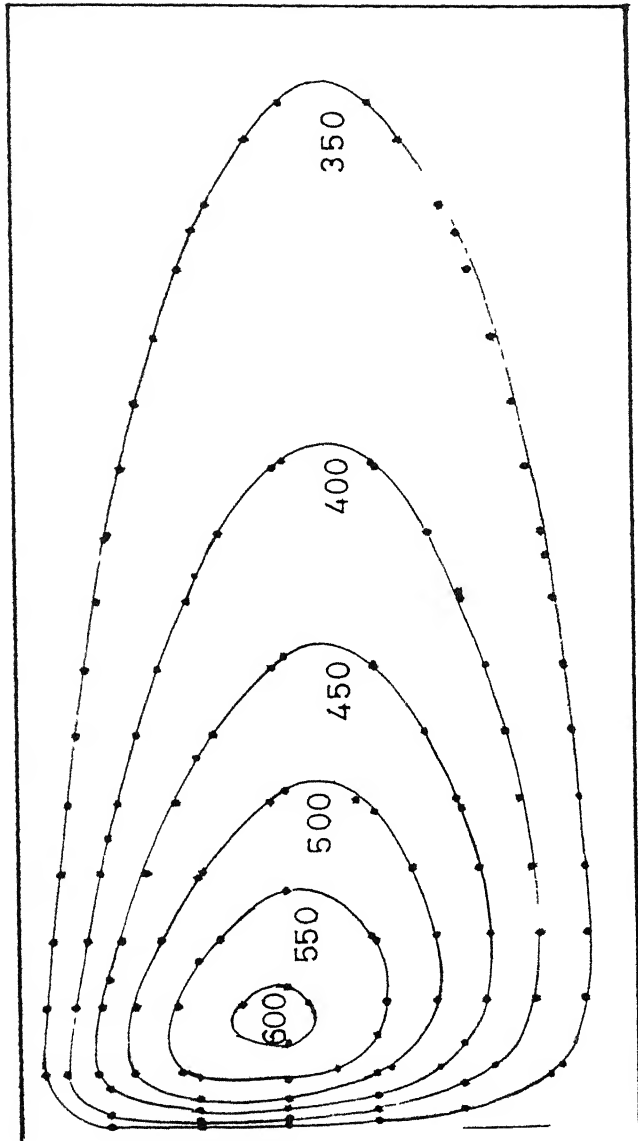


FIG4.4A ISOTHERMS FOR 119 ELEMENT GRID

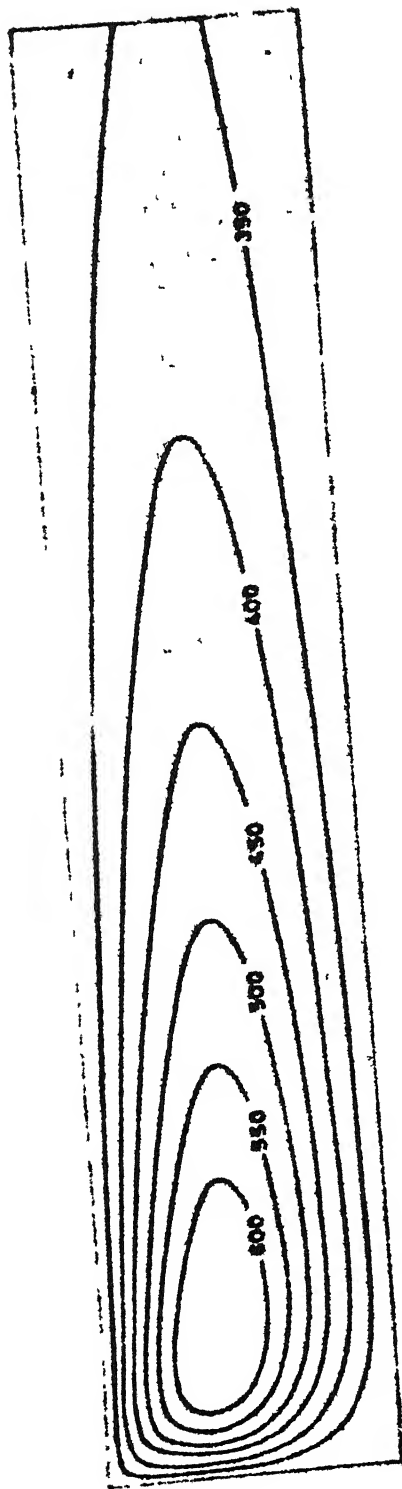


FIG. 4.4B : ISOTHERM PLOT FROM REFERENCE [9]

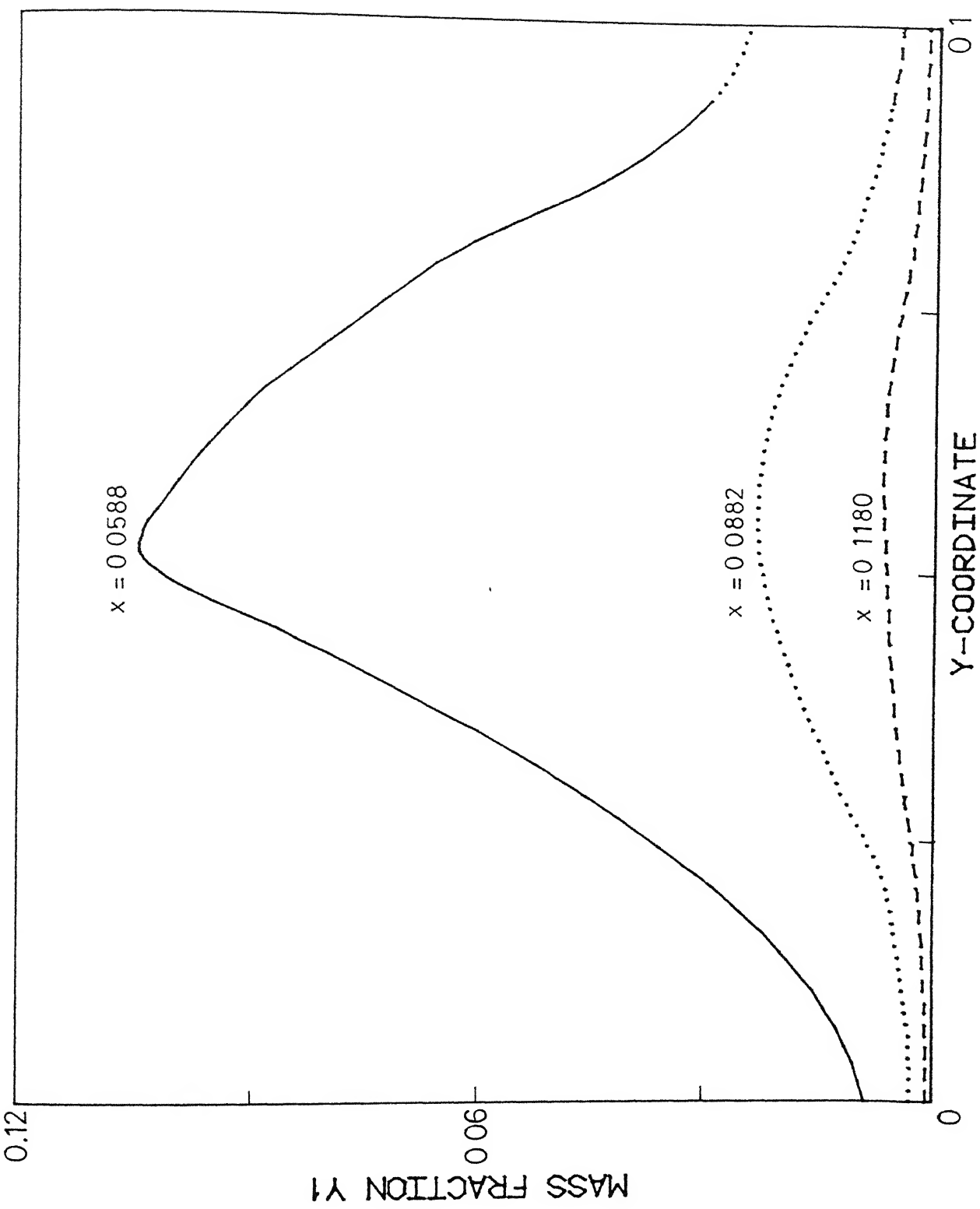


FIG4.5 Y1 PROFILE PLOTTED FOR 40 ELEMENT ADAPTED GRID

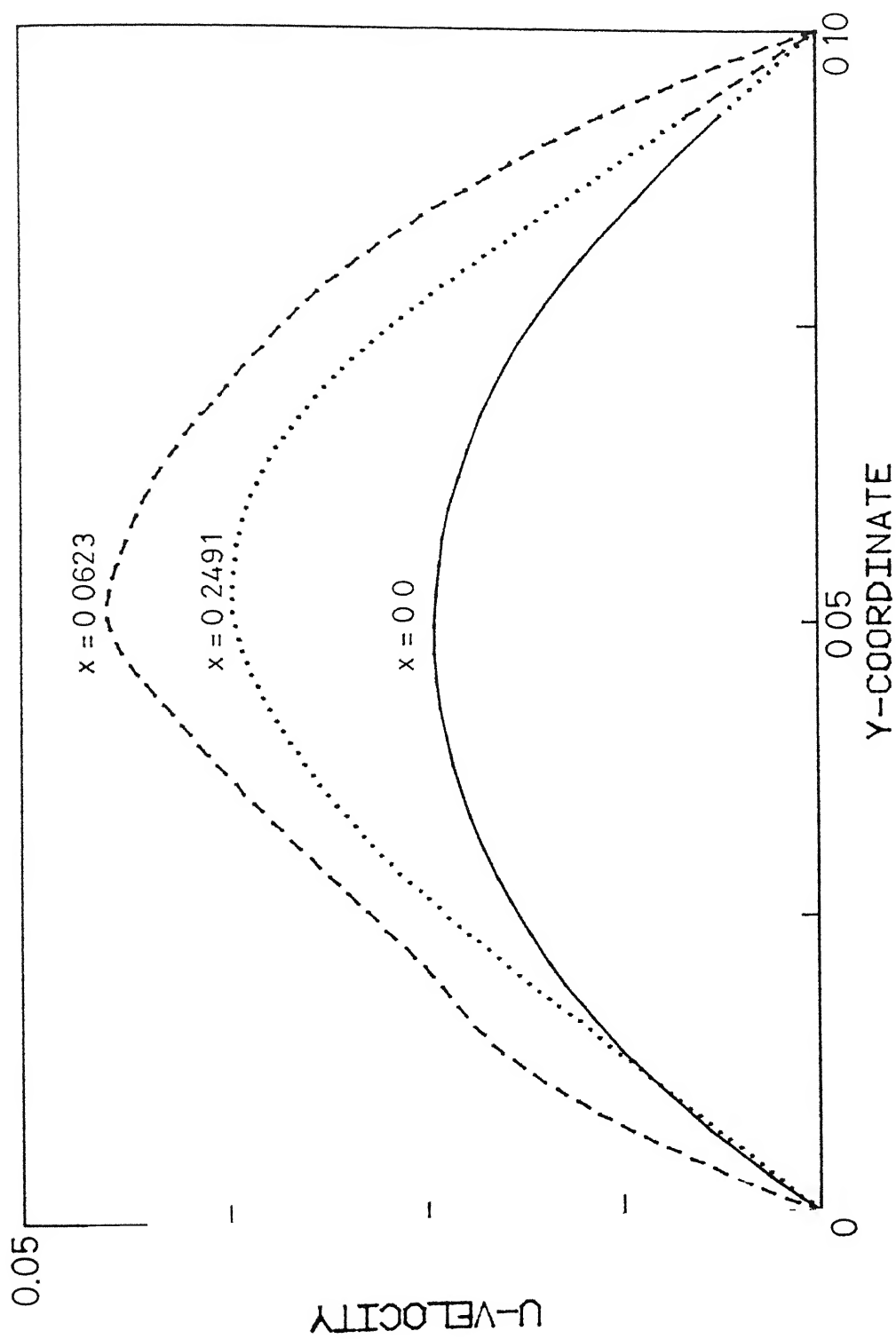


FIG4.6 U-VELOCITY PROFILE PLOTTED FOR 40 ELEMENT ADAPTED GRID

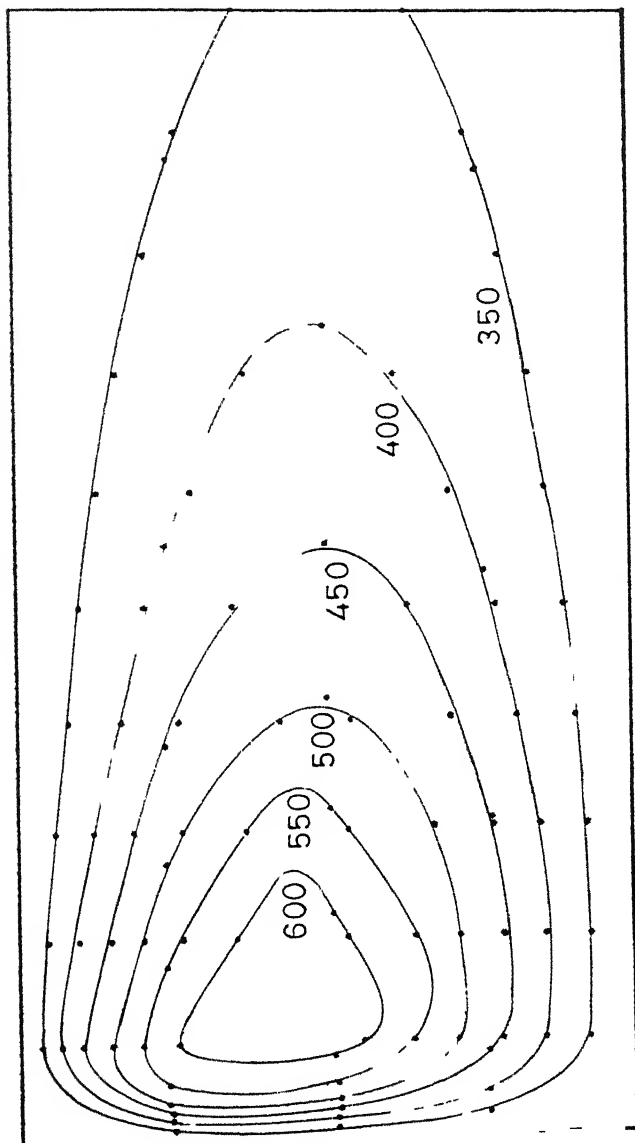


FIG47 ISOTHERMS FOR 40 ELEMENT ADAPTIVE GRID.

CENTRAL LIBRARY  
Kanpur

Acc. No. **A** 99723

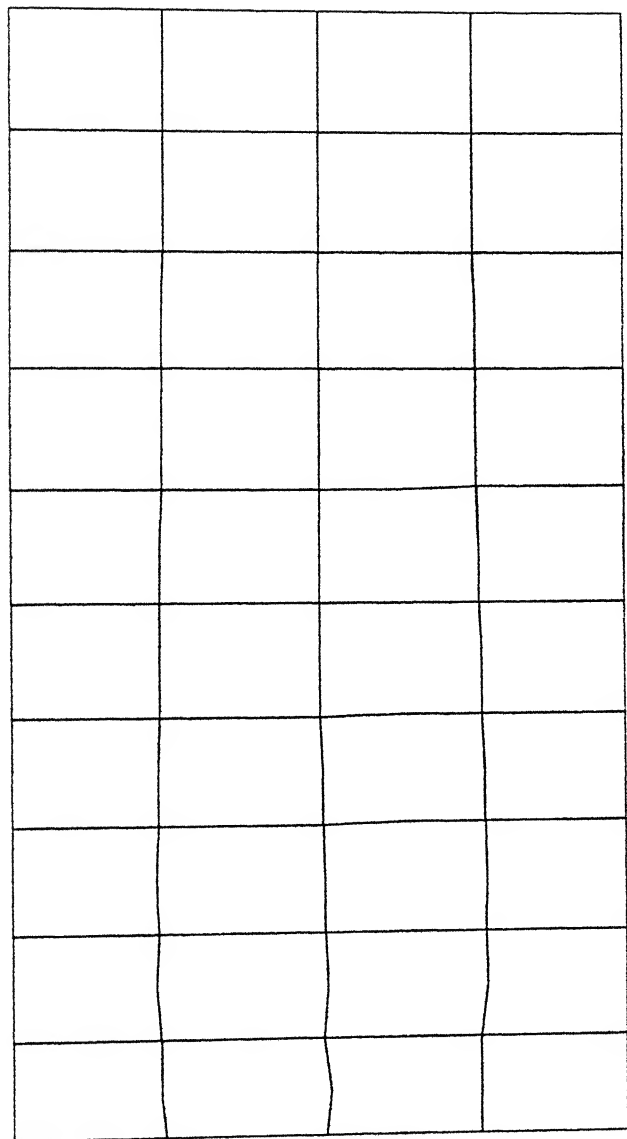


FIG 4 8 GRID STRUCTURE AFTER 6TH ADAPTATION

## CHAPTER 5

The third problem solved by the application of the adaptive finite element technique is the Blasius problem of boundary layer flow over a flat plate Fig. (5.1). Apart from the velocity boundary layer, the thermal boundary layer has also been included for analysis.

The physical description of the problem is as follows. A viscous fluid flows steadily over a flat plate at zero incidence. The flow is laminar and there are no pressure gradients in the flow direction. Heat transfer occurs due to an applied temperature difference between the fluid and the plate. The equations governing the flow and the heat transfer (for incompressible flow):

$$\frac{\partial u}{\partial x} + \frac{\partial v}{\partial y} = 0 \quad (5.1)$$

$$u \frac{\partial u}{\partial x} + v \frac{\partial u}{\partial y} = \mu \frac{\partial^2 u}{\partial y^2} \quad (5.2)$$

$$\rho C_p u \frac{\partial T}{\partial x} + \rho C_p v \frac{\partial T}{\partial y} = \frac{\partial}{\partial y} \left( k \frac{\partial T}{\partial y} \right) \quad (5.3)$$

where  $\rho$ ,  $C_p$ ,  $k$ , are constants and are specified for the solution of  $u$ ,  $v$  and  $T$  and  $y \ll x$ .

Using

$$\bar{x} = x/L$$

$$\bar{y} = y/\delta$$

$$\bar{u} = u/U_\infty$$

$$\text{and} \quad \bar{T} = T/T_{\infty} \quad (5.4)$$

the dimensionless governing equations, after dropping the bars over the non-dimensional quantities for convenience, become

$$\frac{\partial u}{\partial x} + \frac{\partial v}{\partial y} = 0 \quad (5.5)$$

$$u \frac{\partial u}{\partial x} + v \frac{\partial u}{\partial y} = \frac{\partial^2 u}{\partial y^2} \quad (5.6)$$

$$u \frac{\partial T}{\partial x} + v \frac{\partial T}{\partial y} = \frac{1}{Pr} \frac{\partial^2 T}{\partial y^2} \quad (5.7)$$

#### NUMERICAL SOLUTION:

Although a simple similarity solution exists for this problem, a finite element numerical solution using a uniform mesh has also been obtained in order to bring forth the advantages of adaptation. The FEM procedure is based on the Galerkin weighted residual approach. The residue equations are obtained as follows:

$$\sum_1^{ne} \iint_{\Omega} \phi_i \left( \frac{\partial u}{\partial x} + \frac{\partial v}{\partial y} \right) d\Omega = 0 \quad (5.8)$$

$$\begin{aligned} \sum_1^{ne} \iint_{\Omega} \left[ \phi_i v \frac{\partial u}{\partial x} + \phi_i v \frac{\partial u}{\partial y} + \frac{1}{Pr} \frac{\partial \phi_i}{\partial y} \frac{\partial u}{\partial y} \right] d\Omega \\ = \sum_1^{ne} \oint_{\Gamma_2} \phi_i \frac{\partial u}{\partial y} d\Gamma_2 \end{aligned} \quad (5.9)$$



$$\begin{aligned}
& \sum_{i=1}^{ne} \iint_{\Omega} \rho_i u \frac{\partial T}{\partial x} + \rho_i v \frac{\partial T}{\partial y} + \frac{\partial \rho_i}{\partial y} \frac{1}{\rho R} \frac{\partial T}{\partial y} d\Omega \\
& = \sum_{i=1}^{ne} \oint_{\Gamma_2} \rho_i \frac{\partial T}{\partial n} d\Gamma_2 \quad (5.10) \\
& i = 1, 2, \dots, 8
\end{aligned}$$

#### BOUNDARY CONDITIONS:

On the flat plate the velocities are equal to zero due to no slip condition. The temperature or flux, ~~is~~ is specified at the flat plate (or wall). In the far stream the  $u$  velocity becomes equal to the free stream velocity and similarly  $T$  is equal to  $T_{\infty}$ . At the leading edge  $u$  and  $T$  are free stream values and  $v$  is equal to zero. Since the equations are parabolic the down stream conditions need not be specified. These are shown in Fig. (5.1).

The results for the FEM solution of the equations are plotted in Fig. (5.2) along with the Blasius series solution for comparison.

#### ADAPTATION:

Adaptation in this problem is carried out in two different ways. Once the grid is moved according to the gradients of  $u$  and another time the basis is temperature.

In both the cases the uniform grid solution, adapted grid solution and Blasius series solution are plotted. In

Fig. (5.2) and Fig. (5.3) the  $u$ -velocity profile for the  $u$ -adapted and  $T$ -adapted solutions are presented respectively. In both the cases the solution accuracy of ' $u$ ' is increased. But Fig. (5.2) shows that the  $u$ -adapted solution gives better result for ' $u$ '.

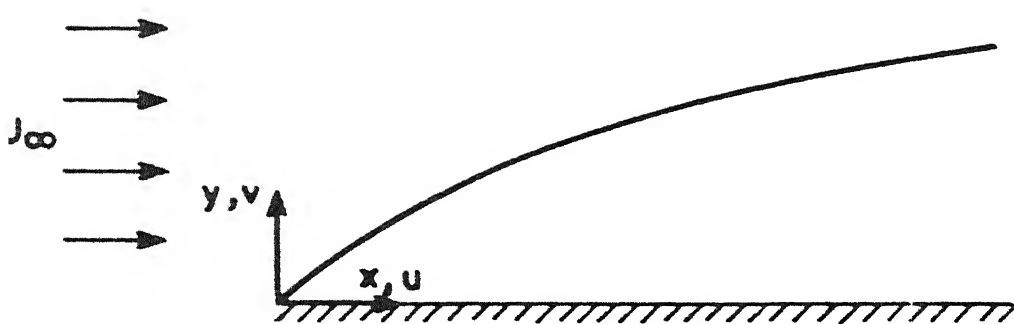


Fig. 5.1 Boundary layer on a flat plate.

Table 5.2

ETA	u uniform grid	u u-adapted grid	u Blasius
0.0	0.0	0.0	0.0
0.4	0.127729	0.130326	0.13277
0.8	0.2557	0.261670	0.26477
1.2	0.3806	0.389625	0.39378
1.6	0.5	0.512254	0.51676
2.0	0.6121	0.625445	0.62977
2.4	0.711	0.725592	0.72899
2.8	0.796	0.809606	0.81152
3.2	0.864	0.875982	0.87609
3.6	0.915	0.92490	0.92333
4.0	0.951	0.95830	0.95552
4.4	0.975	0.976	0.97587
4.8	0.988	0.989	0.98779
5.2	0.989	0.991	0.99425
5.6	0.993	0.994	0.99748

Table 5.3

ETA	u uniform grid	u T-adapted grid	u Blausius
0.0	0.0	0.0	0.0
0.4	0.127729	0.12864	0.13277
0.8	0.2557	0.2577	0.26477
1.2	0.3806	0.3839	0.39378
1.6	0.5	0.5047	0.51676
2.0	0.6121	0.6166	0.62977
2.4	0.711	0.7163	0.72899
2.8	0.796	0.8	0.81152
3.2	0.864	0.868	0.87609
3.6	0.915	0.919	0.92333
4.0	0.951	0.954	0.95552
4.4	0.975	0.976	0.97587
4.8	0.988	0.990	0.98779
5.2	0.989	0.992	0.99425
5.6	0.993	0.993	0.99748

CONCLUSIONS AND SUGGESTIONS

1) The applicability of the present adaptation technique has been demonstrated by the three physical problems considered. The problems are two-dimensional but correspond to diverse applications which promises the use of this technique to a wide range of two-dimensional problems. It is easily possible to extend the method to three dimensional cases also.

2) This technique is particularly useful in the case of non-linear problems like the test problem of chemically reacting laminar flows. Adaptation is carried out after each iteration to successively improve upon the prediction of the solution variables in the large gradient regions.

3) The weight constant 'W' should be a large value to retain the extremum properties of the elliptic generation system.

If the extremum principles are violated the resulting grid may be too much skewed and in some cases the interior nodes shoot out side the boundary which is not allowed,

4) Finally it is shown that this adaptive finite element technique has several advantages over the other adaptive grid methods as explained below:

(a) The technique is best suited for coupling with the finite element method which is used widely nowadays. Standard finite element routines are used in the present work and so the software is very simple.

(b) The adaptation is carried out all over the domain in one stroke unlike the line by line or series of one-dimensional adaptations followed in the attraction repulsion scheme or the spring analogy. So the gradients are sensed all over the domain at the same time and accordingly the points are moved.

(c) The presently available grid adaptation methods are primarily meant for finite difference solutions and so complicated transformations of governing equations of the problems are necessary to carry out computations in the orthogonal domain. Such complex transformations are not required in the case of finite elements.

(d) The automatic mesh refinements schemes available for finite elements increase the computational time for numerical simulation. Another disadvantage with those schemes is that the grid is not dynamically adapted. Considerable user interaction is necessary

The present scheme is dynamically adaptive and it does not refine the grid by adding more elements. So computational time does not increase very much.

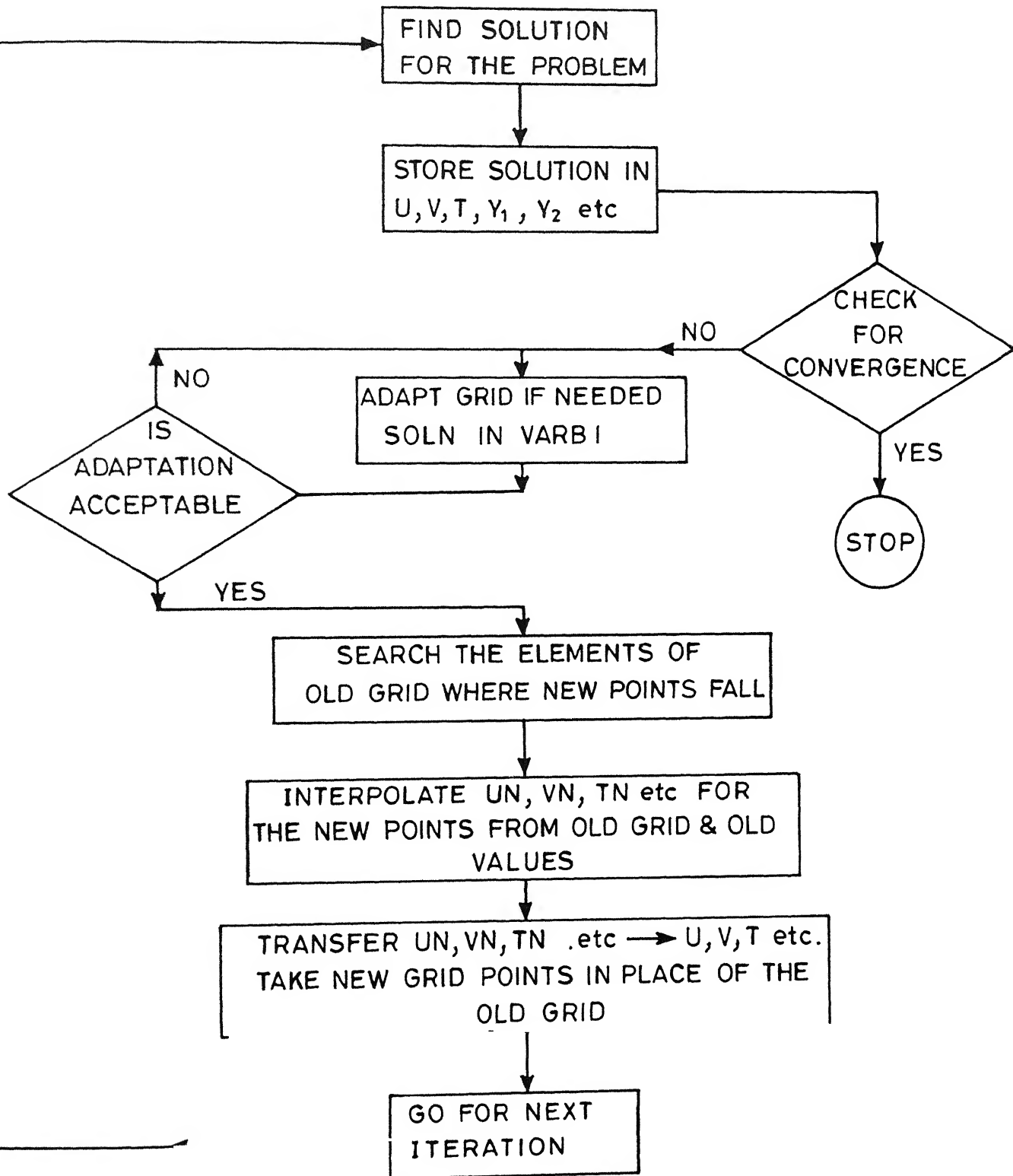
#### SUGGESTIONS:

- 1) In the present work, the first derivative is taken as the control function, with the sign of second derivative for controlling the direction of node movement. More detailed study is necessary for the selection of appropriate control functions.
- 2) A curvature term as indicated by Thompson J.F. [8] can be taken along with the first derivative, to avoid ~~disturbance~~ clustering of nodes near sharp corners.
- 3) In case the original mesh is not suitable for the physical problem the adaptation may compound the difficulties and severe oscillations may occur in the solution. So techniques must be developed to provide a good initial mesh.
- 4) The weight constant 'W' should be based on some grid properties such as maximum/minimum spacing between nodes or maximum/minimum angle between grid lines.



## APPENDIX A

For adapting the mesh in a particular physical problem the programme is stored in three files, for convenience. The first file is the original problem code which finds the solution of the problem for coarse grid. The solution is checked for convergence. If the adaptation is to be carried out then subroutine LINKGRD in the second file is called. This file adapts the mesh and if the new mesh is acceptable it calls the INTPOL routine which is in the same file. The routine INTPOL interpolates the values of the variable(s) to the new grid points. This interpolation is carried out on the basis of the previous grid and the previous variable values. These interpolated values become a part of the iterative procedure for the main problem. After this operation the routine substitutes the new grid coordinates in place of the previous values and returns the new grid to the main problem and again the solution procedure is carried out. The third file contains the general routines used in finite elements like SHAPE8, DJACOB, SURFIN, FRONTS etc. which can be referred in [10]. The flow chart for the procedure mentioned above can be seen in Appendix B.



Flow chart for adaptation

## REFERENCES

1. Dwyer, H.A., Kee, R.J. and Sanders, B.R., "Adaptive Grid Method for Problems in Fluid Mechanics and Heat Transfer", AIAA Journal, Vol. 18, No. 10, October 1980.
2. Brackbill, J. and Saltzman, J., "Applications and Generalizations of Variational Methods for Generating Adaptive Meshes", Numerical Grid Generation, Ed. J.F. Thompson, North-Holland, 1982, pp. 865-884.
3. Anderson, D.A. and Rai, M.H., "The Use of Solution Adaptive Grids in Solving Partial Differential Equations", Ed. J.F. Thompson, North-Holland, 1982.
4. Gnoffo, P.A., "A Finite-Volume, Adaptive Grid Algorithm Applied to Planetary Entry Flow Fields", AIAA Journal, Vol. 21, No. 9, September 1983.
5. Nakahashi, K. and Deiwert, G.S., "A Self Adaptive Grid Method with Application to Air Soil Flow", AIAA Paper 85 - 1525 - CP, July 1985.
6. Das, A.K., "Adaptive Grid Generation and Its Applications", M.Tech. Thesis, Department of Mech. Engg., IIT Kanpur, August 1986.
7. Berger, M.J., Jameson Antony, "Automatic Adaptive Grid Refinement for the Euler Equations", AIAA Journal, Vol. 23, No.4, April 1985.
8. Thompson, J.F., "Numerical Grid Generation", North-Holland, 1985.
9. Winters, K.H. et al., "The Finite Element Method for a Laminar Flow with Chemical Reaction", Int. J. for Num Methods in Engg., Vol. 17, 1981, pp. 239-253.
10. Taylor, C., Hughes, T.G., "Finite Element Programming of the Navier-Stokes Equations", Pineridge Press Limited, Swansea, UK, 1981.
11. Reddy, J.N., "An Introduction to the Finite Element Method", International Student Edition, McGraw-Hill Book Company.

14 99723

Thesis

621.40220154 Date Slip 99723

K897n

This book is to be returned on the  
date last stamped

ME-1987-M- KRI-NOV